



Flinders
UNIVERSITY

**Online Optimization of Adaptive
Vibration Control System of
Dynamically Loaded Flexible
Structures**

by

Guangyang Chen, M.Eng. (Electronics)

Date of submission: May 2018

Submitted to the College of Science and Engineering in partial fulfilment of the requirements
for the degree of Master of Engineering (electronics)

Declaration

I certify that this work does not incorporate without acknowledgment any material previously submitted for a degree or diploma in any university, and that to the best of my knowledge and belief it does not contain any material previously published or written by another person except where due reference is made in the text.

Guangyang Chen

Signature: 

Date: 29/08/2018

Acknowledgement

First, I'd like to say thank you to my supervisor, Fangpo He, I'm inspired by her dedicated work style and encouraging persistence. I really appreciate her valuable input and encouragement to this challenging project.

And I'm thankful to Ph.D. student Peng Zhang, for his generosity in helping me during the project.

Also, I want to say thank you to all related staff that helped a lot in many ways, thank you for your patience and kindness.

Finally, special thanks to my wife, thanks for your selfless support all the way.

Abstract

Many physical systems to be controlled are time-varying in nature, i.e., the system parameters will change according to different operating conditions. This is certainly true for a dynamically loaded flexible structure in which system parameters, such as natural frequencies, are functions of the structure loading conditions. In this circumstance, an adaptive control system will be needed to provide a consistent system performance over a wide range of operating conditions. Different from a non-adaptive control system, an adaptive control system must be able to work with unknown structural parameters and must provide a satisfactory control effect with a fast time response.

In this project, a multi-input multi-output (MIMO) vibration cancellation control system is developed for a dynamically loaded plate structure to remove its single and multiple modes of vibrations caused by unwanted disturbances. The adaptive MIMO control system is constituted by an online parameter estimator and an adaptive controller. With appropriately estimated parameters supplied by the online parameter estimator, the adaptive controller will be able to control the system successfully. Positive position feedback (PPF) that offers a fast roll-off at high frequencies is chosen to construct the adaptive controller. The stability of the resulting closed-loop system is guaranteed with high robustness.

Since the design of the controller depends on a validated mathematical model of the system, a MIMO system identification is conducted via experiment. Only the first three modes of the system are considered to be within the frequency range of concern. The experimental setup is constituted by a top plate supported by three pairs of sensors and actuators that are connected to a base plate. The base plate is shaking consistently by a disturbance transducer that introduces a disturbance signal into the system. By using curve fitting techniques, a transfer function matrix of the MIMO plate structure is obtained.

A most recognized challenge in an adaptive controller design lies in the optimization of the controller parameters. For online control of a time-varying system, the controller parameters need to be updated whenever a change in the system operating condition occurs. Online controller parameter optimization thus presents the biggest challenge in fulfilling the required control goal with unknown operating conditions. Computation of real-time optimization of controller parameters requires a large amount of computational time with high computation power and is often considered as unachievable in real-time implementations.

In this project, a sub-optimization method is proposed, in which two optimized PPF controllers are designed off-line for two different working conditions (unloaded and fully-loaded). When an unknown working condition is observed and estimated by the online parameter estimator, one of the two pre-designed PPF controllers will be applied to the system temporarily to control the unknown condition, while a new PPF controller will be optimized online within a required period of time to replace the pre-designed controller.

To achieve this, a mathematical model of the current working condition is first generated by online parameter estimation. The vibration frequency is estimated by a frequency estimator. A linear relation is assumed for mode shape prediction purpose. For each one mode, the mode shape is changing linearly subject to the change of the natural frequency. The damping ratios of the unknown working condition are selected to be the same as either the unloaded or the fully-loaded condition based on which frequency is closer to the unknown working condition. Secondly, according to the structure of the MIMO PPF controller, the compensator frequency matrix, damping matrix, and gain matrix are the compensator parameters that need to be designed. For the purpose of active damping, the frequency matrix is set to be equal to the natural frequency matrix of the structure. The damping ratio matrix of the pre-designed PPF controller is used as the damping matrix for the unknown working condition due to high robustness of the PPF controller. Thus, the only compensator parameter that needs to be optimized is the gain matrix. Subsequently, an H_∞ norm of the closed loop frequency response function is defined for the optimization purpose. Then, two optimization methods are proposed, the Genetic Algorithm (GA) method and the Simulated Annealing (SA) method. For the GA method, the computational time is mainly related to the size of population and the number of generations. To ensure the population diversity, the size of population cannot be largely deducted. However, by setting different Probability of Performing Crosser and Probability of Mutation for two fitness levels (under average and over average), the number of generations can be reduced. For the SA method, normally, the initial value of the optimization parameter is chosen randomly. However, for saving time purpose, the initial value is selected to be the value of the chosen pre-designed PPF controller. In principle, although the GA method can provide a very accurate optimization result, it costs more time. On the contrary, the SA method requires less time, but possesses a limited ability to find the most accurate optimization result.

To propose the sub-optimization step, two optimized MIMO PPF controllers are designed off-line for the unloaded and fully-loaded conditions, respectively, and the simulation results validate the effectiveness of both scenarios. Compared with the open-loop frequency response, the closed-loop frequency response can achieve up to 10.347dB attenuation. Then, the simulation of an unknown working condition is carried out in which one of the pre-designed MIMO PPF controllers is used to temporarily control the unknown condition. Simultaneously, the GA and SA methods are used to calculate the optimized parameters of the PPF controller for the unknown working condition online. The frequency matrix and the damping matrix of the adaptive controller are designed in advance, while the gain matrix of the controller is optimized online. To take into account the possible spill-over effect that high frequencies may introduce to low frequencies, the controller gain for the highest mode of concern is optimized first, followed by the gains of the subsequent lower modes of concern. As soon as an optimized gain is generated, the corresponding gain and designed frequency of the adaptive controller are updated. The other parameters of the adaptive controller remain pending, until the whole gain matrix is optimized. Simulation results reveal that a further 5.20 dB attenuation can be achieved by using the SA optimization method in 28.158 seconds, while a further 5.43 dB attenuation is achievable by using the GA optimization method, the total computation time is 428.472 seconds

In conclusion, compared to the traditional GA and SA methods, the proposed modifications, as applied to the online optimization of the underlying MIMO PPF adaptive controller gain matrix, can save a significant amount of computational time. Even though the time consumption is still considered to be high for an effective real-time operation of the MIMO adaptive controller, the proposed method provides a foundation upon which possible means of achieving further reduction of the computational time can be investigated. Nevertheless, this thesis sets up an example of combining an online optimization scheme with an online parameter estimation capability to produce an adaptive control system that is capable of dealing with unknown working conditions of a MIMO time-varying dynamic structure satisfactorily.

List of Figures

Figure 1.1 Laboratory model used in this vibration cancellation project.....	2
Figure 3.3.1 Block diagram of hardware connections.....	10
Figure 4.2.1 Block diagram of PPF control system.....	17
Figure 4.2.2. Block diagram of multi-mode MIMO PPF control closed-loop system.....	17
Figure 4.3.1 Block diagram of SSM control system.....	20
Figure 5.1 Block diagram of GA.....	22
Figure 5.3.1 Block diagram of the SISO single-mode control system.....	28
Figure 5.3.2 Block diagram of the subsystem of controller.....	29
Figure 5.3.3 Responses of the original and pre-designed controller controlled system.....	29
Figure 5.3.4 Computation time of the GA optimization operation.....	29
Figure 5.3.5 Responses of the original and optimized controller controlled system.....	30
Figure 6.3.1 Block diagram of SA algorithm.....	36
Figure 6.3.1 Subsystem of the controller.....	38
Figure 6.3.2 Computation time of the GA optimization operation.....	38
Figure 6.3.3 Responses of the original and optimized controller controlled system.....	39
Figure 7.1 The block diagram of the adaptive control system with online optimization operation.....	40
Figure 7.1.1 The adaptive optimization control system for single-mode configuration.....	41
Figure 7.1.2 The subsystem of the system estimation.....	41
Figure 7.1.3 The subsystem of the online calculation.....	41
Figure 7.1.4 The subsystem of the controller.....	42
Figure 7.1.5 Simulation result of single-mode adaptive control optimization system.....	43
Figure 7.2.1 Block diagram of the control system in the MIMO configuration.....	44
Figure 7.2.2 Block diagram of the controller subsystem.....	44
Figure 7.2.3 Response of the non-optimized control system.....	45

List of Tables

Table 5.1 Control performance SISO single-mode control system optimized via GA.....	30
Table 6.1 Control performance SISO single-mode control system optimized via SA.....	39
Table 7.1 The optimization performance of GA approach.....	49
Table 7.2 The optimization performance of SA approach.....	49

Contents

Declaration.....	ii
Acknowledgement	iii
Abstract.....	iv
List of Figures	vii
List of Tables	viii
Chapter 1 : Introduction	1
1.1 Project Background.....	1
1.2 Experimental Setup	1
1.3 Research Methodology.....	2
1.4 Outline of This Thesis	4
Chapter 2 : Literature Review.....	5
Chapter 3 : System Identification	9
3.1 Structure of Transfer function.....	9
3.2 System Modelling	11
3.3 Differential Equation Derivation.....	17
Chapter 4 : Online Optimization Preparatory Work.....	20
4.1 Time-varying Structure Parameters Estimation	20
4.2 Positive Position Feedback(PPF) controller.....	23
4.2.1 PPF controller structure	23
4.2.2 Parameters of PPF controller pretreatment.....	25
4.3 Sub-optimization step design	26
Chapter 5 : Online Optimization via Genetic Algorithm Approach.....	28
5.1 Genetic Algorithm Theory	28
5.2 Genetic Algorithm Online Optimization Design	29
5.2.1 Initialization.....	30
5.2.2 Fitness Evaluation.....	31
5.2.3 Selection	32
5.2.4 Crossover and Mutation.....	33
5.2.5 Decoding.....	34
5.3 Simulation Construction and Explanation.....	35
Chapter 6 : Online Optimization via Simulated Annealing approach	39
6.1 Simulated Annealing Optimization Theory	39

6.1.1 State expression	39
6.1.2 Neighborhood definition and movement	40
6.1.3 Thermal equilibrium condition	41
6.1.4 Cooling control	41
6.2 Simulated Annealing Procedures Design	42
6.3 Simulation Construction and Explanation	44
Chapter 7 : Conceptual Optimization Validation	47
7.1 Online optimization of the adaptive control system via single-mode configuration	47
7.2 Online optimization of the adaptive control system via multi-mode configuration	51
Chapter 8 : Conclusion	59
Chapter 9 : Future Work	62
9.1 Directly observing evaluation approach	62
9.2 Online optimization via Quadratic optimal control theory	62
Appendix A: MATLAB Code	65
Bibliography	66

Chapter 1 : Introduction

1.1 Project Background

It is known that many industrial equipment and facilities, such as aircraft, robotic arms and lifting gears, are working in a variational condition. The changing working conditions (e.g. variation of the weight fuel tank) may cause changes of their structures. Therefore, adaptive control plays an important role in control system. Based on observations of the time-varying system, adjusting the design of the controllers is the basic principle of the adaptive control. Therefore, a precise observation and an appropriate adjusting scheme can improve the performance of the adaptive control system. Moreover, the optimization is also a key operation because not all of the adaptive controller parameters may not be able to be adjusted directly via the observation of the structure. A successful optimization can save the cost of control and provide a preferable control effect. And a non-optimized controller may cause even opposite control result because some key parameters are not adjusted correctly in the adaptive control system.

In all kinds of control systems, the vibration control system is studied widely with aim of making the target structures stable. When a disturbance signal has frequency, which equals to the natural frequency of the structure, an excessive vibration will appear. This phenomenon is called resonance. Resonance can cause mechanical distortion and dynamic stress to the structure. Nowadays, there exists an obvious trend that mechanical structure becomes more flexible along with the rapid development of material technology and economic considerations. Therefore, in the industrial control systems, resonance control takes an increasingly important position [24].

Hence, this project mainly focuses on the optimization of the adaptive vibration controller via dynamic loaded condition which aims at optimizing the parameters of the adaptive controllers in order to provide an improved control effect.

1.2 Experimental Setup

In this project, the adaptive control system, which is a multi-input multi-output (MIMO) system, is optimized with the aim of vibration cancellation. The target object is a flexible plate. And a

dynamic loaded condition of this structure is considered and set up to provide a time-varying structure.

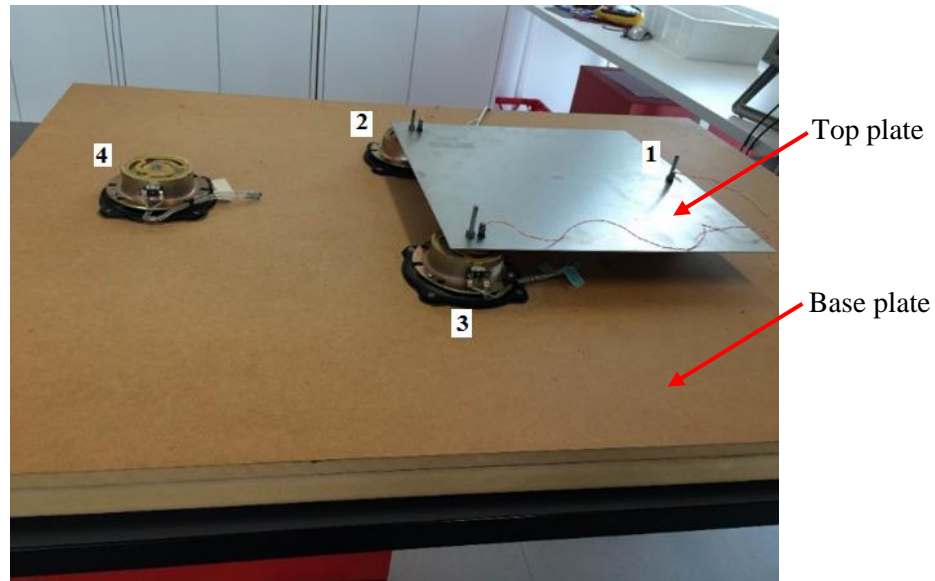


Figure 1.1 Laboratory model used in this vibration cancellation project

As shown in Figure 1.1, the laboratory model is constituted by a base plate, a top plate and 4 transducers (one transducer is used to generate the disturbance and the other three transducers are used as both sensors and actuators). The disturbance generation transducer is mounted on the base plate. The others are fastened with the top plate by screws and their bottoms are fixed on the base plate as well.

The input frequency which is increased from 20 Hz to 60 Hz is applied to Transducer 4 as a disturbance. The range of the frequency is selected based on the natural frequencies (modes) of the experimental plate. With a purpose of fitting the vibration response curve in the frequency domain as accurate as possible, the range of the disturbance frequency is chosen to cover teens of modes for the plate. The vibrational response of the system is measured by three sensors which is fixed on the top the transducers from 1 to 3. The measured signals are fed to the computer to be analyzed by ModalVIEW

1.3 Research Methodology

With a purpose of optimizing the adaptive control system, procedures of dealing with a typical optimization problem were followed.

The first step is to process the system identification. Based on the modelling knowledge, theoretical analysis method is firstly used to build a mathematical expression of frequency

Chapter 1: Introduction

transfer function of the plate. Then, via physical experiment method, the parameters of transfer functions are obtained by using ModalVIEW, a popular modal analysis software. After that, modal truncation is applied for controller design purpose.

The second step is estimation of the system when the loaded condition is changed. There are two exactly same loads are set to provide three different loaded conditions, fully loaded, half loaded and unloaded. The major parameter different between these three conditions is only the amount of the load. When the loaded condition is changed, the natural frequency, damping ratio and the model shape are changed as well. Hence, the estimation of these three parameters is required to proceed. The activated natural frequency of the system is obtained by three band pass filters and a frequency estimator. The frequency range of each band pass filter is designed based on the frequency range of each mode of concern corresponding to a loading condition. The frequency estimator is designed based on Zero-Cross theory. Based on the results of the estimation, the system mathematical model is modified. The natural frequency is firstly estimated. And then the other parameters, damping ratios and mode shaped are selected and calculated by using the estimated natural frequency.

The third step is to establish a sub-optimization system. This step aims at controlling the time-varying plate in a relatively stable condition before the optimization operation is finished. In sub-optimization design section, the adaptive controller is optimized in two loaded condition, unloaded condition and fully-loaded condition. There are two exactly same loads which are set to provide three different loading conditions: fully loaded, half loaded, and unloaded. The major parameter different between any two loading conditions is the amount of the load. The selection of these two controllers depends on the natural frequency of which controller is closer to the estimated nature frequency of the current system.

The fourth step is to apply online optimization. Two methods Genetic Algorithm and Simulated Annealing algorithm are designed based on the specific compensator. With an already estimated structure, the optimization methods are required to be simplified and modified to minimize the optimization time. Finally, these two approaches are validated via a simple system in the MATLAB SIMLINK.

The last step is to further validate optimization effect. The validation is performed in a single-input single-output system. And then, a simulation of the real system is set up to obtain the performance of compensators which are optimized by above two methods, and corresponding online optimization results are analyzed and compared.

1.4 Outline of This Thesis

In this thesis, vibration cancellation of a square aluminum plate structure is presented by using positive position feedback control technique. Thesis outline is revealed as below:

In chapter 2, an overall literature review is given. Main previous works are summarized chronologically. Different estimation methods and various optimization techniques are analyzed and compared.

In chapter 3, the system identification is set up to provide a well mathematical model which is used for the design and optimization of the adaptive controller. Via physical experimental modelling method and theoretical analysis, the identification problem can be solved. And the mathematical model of the time-varying structure can be easily adjusted to match current target structure by estimating some key variables.

In chapter 4, the precondition is performed to make sure the online optimization is able to proceed. The preparation work includes the estimation of the time-varying structure, target parameters selection and determining their range, and the design of sub-optimization step which consists two conditions off-line pre-designed controllers and selection method.

In chapter 5 and chapter 6, the online optimization is performed via Genetic algorithm approach and Simulated Annealing algorithm, respectively. For each approach, the corresponding procedure is build. Moreover, some of steps are modified and simplified with the purpose of saving the computation time. Finally, the verification and simulation of each method are proceeded on the Matlab software.

In chapter 7, two configurations single-mode configuration and multi-mode configuration are constructed for validation. Then, according to the results from the simulations, a summary of these two approaches are built.

In chapter 8, the conclusion from all above experiments was drawn based on this project conclusion and problems encountered during the project.

In chapter 9, future works were suggested. According to the optimization results from the simulation exist shortcomings, two possible developed methods were mentioned.

Chapter 2 : Literature Review

In this chapter, the content includes the reviewed literature about the adaptive vibration control system optimization approaches. With an aim at optimizing a time-varying structure online, the selected controller, Positive Position Feedback (PPF) controller, is required to analyzed firstly. Based on the characteristics of PPF controller, the strategy of online optimization is ensured. The parameters of PPF controller is divided into two parts. For the first part, the parameters are optimized online based on the estimation of the current structure. For the second part, the parameters are required extra optimization operations. The methods of evaluating control performance are then analyzed and compared. For each approach, both advantages and disadvantages are discussed.

In this project, the Positive Position Feedback (PPF) controller is selected as the adaptive controller. The PPF controller is constituted by three parameters, damping, control frequency and gain. According to the PPF control theory, the control frequency is required to designed as same as the natural frequency of the structure. Moreover, the value of the damping can be selected as the original values (the damping values of the off-line optimized PPF controller with unloaded, half loaded and fully loaded conditions) because of the high Robustness of the PPF controller. As a result, the control frequency and damping can be modified directly based on the result of the structure estimation. However, the controller gain is required to be optimized online with extra operations.

The control object is a time-varying structure. By processing an effectual estimation operation, the system can be identified, and its corresponding mathematical model can be defined [35]. Considering the characteristics of structure of this project, the natural frequency estimation is the major part in the first operation. In order to estimating the natural frequency on-line, the Fast Fourier Transform method can be used [19]. Although this method provides a way for estimation online, the experts Proakis and Manolakisi [20] pointed out that this method requires sampled data consist of complete representation all time or repeatably and lost ability to remove the impacts from leakage. Another estimation online method is adaptive filter with neural networks method, but it requires a sensor for every interested mode, converges slowly [21] and represents a single mode system only without neural networks [22]. Another method is Recursive Least-Squares (RLS) method which is studied by Rew, Han and Lee [23]. Their study shows that RLS method gives fast parameter convergence and allows fast adaptation under changing conditions.

Chapter 2: Literature Review

After estimating the natural frequency of the structure, the control frequency and damping can be ensured. Subsequently, the controller gain is required to be optimized. Since there exists a linear relationship between the gain of the controller and control effect, the optimization problem can be regarded as a linear programming problem [1].

For solving the linear programming problem, the most commonly used analytical method in linear programming is the Quadratic program method. Yang and Wang [2] and his group provided the Quadratic program method for online optimization for the fast model predictive control system. For this method, this article provides a warm start way to improve the performance of the system. The warm start method is to create a set of parameters which are used in a high frequency in order to reduce the time of running in the system. In the Quadratic program theory, some experts [3] also discussed the active-set and interior-point methods which are the most common used to optimize online the parameters of the control system. They also said that for time-critical interior-point would take an unacceptable time. Moreover, the active-set also needs to define some necessary parameters and functions of the system based on the active-set method [4], [5] & [6]. Thirdly, the gradient algorithm method is also discussed by the experts Tanguy [7] and his group. For this method, it would highly improve the performance of the system, which is worked for the key parameter 'a'. However, it is related to the characteristics of Adaptive Laguerre-Based Filter. Therefore, it may not be very useful for our system, adaptive MIMO vibration cancellation system. Finally, some other methods, such as augmented Lagrangian and extensions of the simplex algorithm, are also mentioned for online optimization, but they are always used for other systems as computer systems rather than vibration control systems [8] & [9].

For now, the interior-point is the most acceptable method for our system, and the functions for its calculation are also provided in some software. In the article [10], the authors provided the knowledge and information theoretically. For using on the control system, some experts [11] showed that to online optimize an embedded model predictive control (MPC) system by using interior-point method is a useful and fast way, which is also mentioned by other research groups [12].

The other kind of linear programming method, the numerical method, is also available for our system online optimization. The principle of numerical method is that by repeatedly observing the performance of system which is consisted by dynamic parameters which are required to be optimized. In the Intelligent control theory, this type of methods have been widely used to

optimize the system. The procedures of this kind of methods are mentioned by Wang [13]. Firstly, the estimation or identification of the target object is required to perform. Then, the performance evaluation method is selected. Finally, by evaluating and filtering for enough times, the optimized parameters are generated.

One of the most popular optimization methods is Genetic Algorithm(GA). In the article [14], [15] & [16], the experts discussed the performance of this method. GA can process most optimization problems. The reason why GA can be used in most of optimization problems is because it can be applied to all types of systems regardless of their complexities. Effective solving optimization problem via GA requires an accurate fitness measuring method and an appropriate amount of iterations. By modifying some steps, GA can be applied to solve most variable values optimization problem. The shortcomings of GA are also pointed out by Chen [17]. he said that the number of evaluation computing operations is normally greater than other methods. Therefore, more computation time is required via GA method. Another method Simulated Annealing(SA) algorithm is mentioned by Li [18]. He said that SA can search the optimal solutions. Although the optimal solutions may not be globally optimal, but SA is still available for optimizing vibration control system.

As two commonly used optimization approaches, GA and SA both have their own advantages and disadvantages. In terms of abilities for global reaching, GA shows higher performance than SA. However, due to requiring enough number of iterations, GA needs more computation time than SA. Therefore, both of GA and SA are studied, verified and compared.

The evaluation methods selection is also important. With the purpose of providing the maximal cancellation of the vibrations, the evaluation results, such as vibration energy and maximal amplitude, are related to the eigenvalue of vibration. The expert Du [24] chooses the vibration energy function as his evaluation function. But he also mentioned that although this function can correctly represent the control effect, the quantity and complexity should not be ignored; therefore, he simplified the calculation evaluating function with a cost of lower accuracy. The M norm is used by Yuan [25] to evaluate the performance of control. By using the M norm to represent the control effect, multiple parameters can be considered at same time, but the computation time has a sharply increasing trend when the number of the parameters rises. Expert Luo and his group [26] deeply discussed different evaluation methods, and they supported that the H norms can be widely used to evaluate the performance of controllers. they also pointed out that different kinds of H norms can represent different properties of the control

system. Also, for the MIMO system, it also shows a well evaluation performance. Some experts, Hu [27] and Chen [28], evaluated the control performance by observing the physical quantities from their experimental equipment. The most significant advantage is breaking away from the limitation of the estimation of target structure. However, it has a higher requirement on the sensors. Also, the observed signals should be disposed when the disturbance from the environment is considered.

The challenges mentioned by Lu [29] are that if the online optimization does not cover all impacts from the disturbances and environment, the speed or performance will be reduced. Like the group of Lu, other experts also showed shortcomings of using online optimization theoretically and directly [30].

According to the literature reviewed above, the current online optimization of controller parameters is only limited to simple controller cases, such as PID (Proportional differential integral) or simple SISO (Single Input Single Output) controllers. In terms of MIMO vibration control systems, especially MIMO PPF control systems existing in the literature, the optimization has been performed offline. Therefore, the online optimization for a time-varying control system is worthy to be studied to provide an effect adaptive control system.

Chapter 3 : System Identification

Since the design of the controller depends on a mathematical model of the system, a validated identification of this MIMO system is requisite. The system is identified via physical experiment modelling method and ModalVIEW software. Finally, the system is represented in the differential equation form.

In this project, the disturbance signal, generated by a transducer, travels through the base board to the other three transducers and finally onto the top plate. The last three transducers are used as both sensors and meanwhile actuators. Therefore, this system is considered as a MIMO system with three inputs and three outputs. The input signals are the vibration forces generated by these transducers, and then the vibration amplitudes of the points, right above corresponding transducers, are read as the output signals.

Based on the input signals and outputs signals, the system will be identified through physical experiment modelling operation. By using ModalVIEW, which is one of the most common modal analysis software, the 3x3 frequency response function (FRF) matrix of the system is obtained. And parameters, natural frequencies, damping ratios, and mode shapes, of each FRF can be defined as well. Finally, in order to calculate the parameters' range of the variable-parameter Positive Position Feedback (PPF) controller, the FRF is required to be derived into differential equation form.

3.1 Experimental Setup

In this section, the experimental setup and the procedure of the experiment are described. The entire physical setup utilized in this project can be divided into four parts. The plate system itself is used to simulate a MIMO vibration problem. Interface board is set to communicate with transducer and dSPACE. NI DAQ 9234 is used for data acquisition for ModalVIEW software. The last one, dSPACE module, is used to compute and generate control signals. The plate system includes plate itself and other equipment: signal generator, oscilloscope, accelerometer and signal amplifier were used to implement the measurement.

A standard sine wave signal with $V_{p-p} = 250\text{mV}$ was generated by the signal generator and amplified by the current amplifier before being applied to transducer i ($i = 1, 2, 3$) as an input signal. The output signal was captured by an accelerometer mounted right above each transducer, amplified by a signal amplifier, and finally shown on the oscilloscope screen.

Chapter 3: System Identification

Change frequency of the sine wave signal from 20 Hz to 60 Hz by increase 0.1 Hz each time. Via the software, ModalVIEW, the input of the MIMO system and the outputs (from there transducers) can be obtained. The input signal and the output signals of each transducers are shown in figure 3.1.1

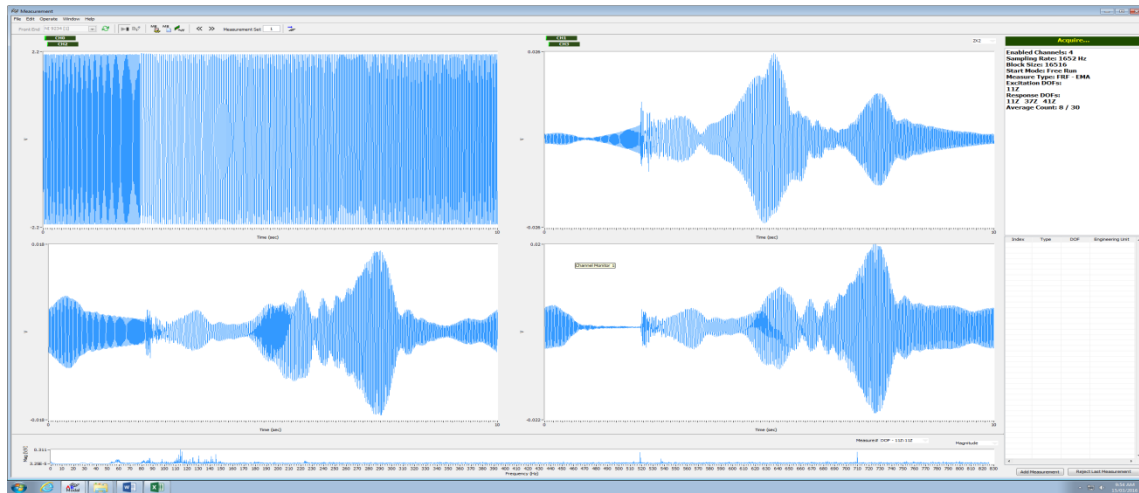


Figure 3.1 Input and output signals

Based on these input and output signals, the ModalVIEW software can change them from time domain to frequency domain, which generates the Frequency Response Function curves.

Firstly, the ModalVIEW software is used to change signals from time domain to frequency domain in order to generate the Frequency Response Function curves. Then, the mode parameters are required to be set. The parameters including the number of modes and extra terms are set by checking the “show FRF fit” option. Thirdly, by clicking “estimate” button, the mode information will appear in the result area. In this area, only natural frequency and damping ratio of each mode can be seen. To obtain more information, the estimation result is required to be saved in a file. After that, the information including natural frequency, damping ratio, magnitude, and phase of each mode can be finally found in the “xxx.mod” file

3.2 Structure of Transfer function

In this section, the structure of transfer function is established according to the theory of control system [35].:

$$Y(s) = G(s) * U(s) \quad (3.2.1)$$

Y(s)-output signal matrix

U(s)-input signal matrix

G(s)-plant dynamics

Chapter 3: System Identification

Due to the fact that the system in this project is a MIMO system, the equation (3.2.1) is rewritten as equation (3.2.2)

$$\begin{bmatrix} y_1(s) \\ y_2(s) \\ y_3(s) \end{bmatrix} = \begin{bmatrix} G_{11}(s) & G_{12}(s) & G_{13}(s) \\ G_{21}(s) & G_{22}(s) & G_{23}(s) \\ G_{31}(s) & G_{32}(s) & G_{33}(s) \end{bmatrix} * \begin{bmatrix} u_1(s) \\ u_2(s) \\ u_3(s) \end{bmatrix} \quad (3.2.2)$$

$y_i(s)$ ($i = 1, 2, 3$)-three output signals

$u_i(s)$ ($i = 1, 2, 3$)-three input signals

$G_{mn}(s)$ ($m = 1, 2, 3$ and $n = 1, 2, 3$)-transfer functions related to m th output and n th input.

Based on the developed analytical derivation of transfer function for this plate [35], the mathematical expression of transfer function for the first three modes is defined as:

$$G_{ij}(s) = \sum_{i=1}^3 \frac{\varphi_{ij}^n}{s^2 + 2\zeta_{ij}^n \omega_{ij}^n + \omega_{ij}^{n2}} \quad (3.2.3)$$

i -the number of outputs

j -the number of inputs

n -the order of mode

φ - the eigenvector (mode shape)

ζ -the damping ratio

ω -the natural frequency

As mathematical expression of transfer function is found, next step of work is to obtain the parameters of transfer function. After obtaining parameters by using modal analysis software, ModalVIEW, the frequency transfer function matrix can be found.

3.3 System Modelling

The structure modelling via physical experiment is supported by 5 major hardware: Signal Generator, Current Amplifier, Transducers, Signal Acquisition Module and PC (ModalVIEW software). The hardware for signal acquisition module is selected as NI DAQ 9234 which is a

4-channel dynamic signal acquisition module and always used for high-accuracy audio frequency data acquisition.

To obtain the FRF in frequency domain, a time-varying frequency, from 20 HZ to 200 HZ signal is generated by the Signal Generator and then amplified by the Current Amplifier. The amplified time-varying signal flew into both the three transducers as exciting signal and the first channel of NI DAQ9234. the output signals of plate are obtained by these three transducers as well. Then the obtained signals are connected to NI DAQ9234 with channels from 2 to 4. Finally, the signals acquired from these four channels are sent to the PC and analyzed by ModalVIEW software.

The block diagram of hardware connections is shown in Figure 3.3.1.

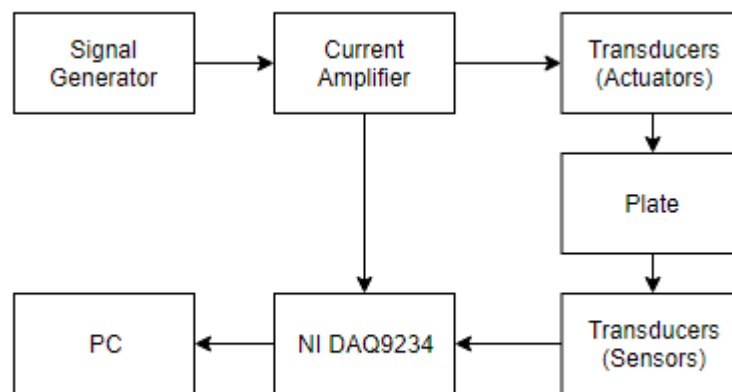


Figure 3.3.1 Block diagram of hardware connections

By using the ModalVIEW software, all of FRF curves are obtained which is shown in figure3.3.2.

Modal analysis result by using ModalVIEW software are listed in Table 3.1. In Table 3.1, 1Y, 2Y and 3Y represent to transducer 1, 2, 3. 2Y:1Y means input from 1Y (transducer 1) output from 2Y (transducer 2). Others are defined in the same way.

Table 3.1 Modal analysis result

Input from transducer 1				1Y : 1Y	2Y : 1Y	3Y : 1Y
Index	Frequency (Hz)	Damping (%)	Shape Type	magnitude	magnitude	magnitude
0	22.26	2.11	Residue Shape	0.00734121	0.00623846	0.00790573
1	27.84	1.924	Residue Shape	0.0404406	0.00213116	0.00704695
2	29.16	1.036	Residue Shape	0.00695505	0.00779947	0.0079244

Chapter 3: System Identification

3	34.79	1.866	Residue Shape	0.0228629	0.0361383	0.0426454
4	42.03	1.768	Residue Shape	0.000872615	0.003148	0.00337096
5	43.77	1.842	Residue Shape	0.00246116	0.0161142	0.0141889
6	49.67	-0.00854	Residue Shape	3.83E-05	9.20E-06	2.15E-07
7	53.7	1.047	Residue Shape	0.0675787	0.0291909	0.0328873
8	58.06	1.458	Residue Shape	0.124132	0.0871378	0.0645218
9	85.62	0.2173	Residue Shape	0.00012324	0.00069505	0.00364918
10	124.7	0.3444	Residue Shape	0.0252533	0.00122437	0.0013487
11	147.2	0.5374	Residue Shape	0.00195614	0.00427431	0.00830553
12	148.2	1.534	Residue Shape	0.0053848	0.0114359	0.013082
13	176.3	0.5288	Residue Shape	0.00478862	0.00650253	0.00648526
14	179.1	0.5678	Residue Shape	0.0160113	0.0207087	0.00316221
15	189.7	0.5049	Residue Shape	5.55E-05	0.00206845	0.0006544
Input from transducer 2				1Y : 2Y	2Y : 2Y	3Y : 2Y
Index	Frequency (Hz)	Damping (%)	Shape Type	magnitude	magnitude	magnitude
0	22.36	2.33	Residue Shape	0.00511256	0.0047365	0.00491893
1	27.68	1.559	Residue Shape	0.00727462	0.00142457	0.00247211
2	29.01	1.489	Residue Shape	0.0116428	0.0231798	0.0251961
3	32.95	-0.4644	Residue Shape	3.98E-05	0.000137	0.00011119
4	34.72	2.612	Residue Shape	0.0513296	0.0747005	0.0868091
5	40.36	2.708	Residue Shape	0.00308732	0.022949	0.0292004
6	43.01	2.635	Residue Shape	0.0210864	0.111906	0.0995804
7	47.26	-1.242	Residue Shape	0.00028949	0.0008129	0.00025496
8	49.85	0.01635	Residue Shape	1.11E-05	1.20E-05	2.85E-05
9	53.55	0.7323	Residue Shape	0.0314204	0.0167561	0.0173905
10	58.23	1.117	Residue Shape	0.0688694	0.0474745	0.0338544
11	85.69	0.243	Residue Shape	0.00101917	0.00365656	0.0214477
12	87.77	0.2926	Residue Shape	0.000391137	0.00142646	0.00067802
13	111.3	1.717	Residue Shape	0.000378693	0.00042752	0.00060699
14	124.6	0.3087	Residue Shape	0.014731	0.00063531	0.000791779
15	147.4	0.763	Residue Shape	0.000872607	0.00461431	0.00708143
16	154.3	0.6028	Residue Shape	0.00381132	0.00780258	0.00122142
17	176.3	0.5722	Residue Shape	0.0048449	0.00643959	0.00663882
18	179.2	0.596	Residue Shape	0.0114811	0.0147498	0.00239068
19	189.3	0.4941	Residue Shape	0.00107498	0.0123975	0.00362142
Input from transducer 3				1Y: 3Y	2Y : 3Y	3Y : 3Y
Index	Frequency (Hz)	Damping (%)	Shape Type	magnitude	magnitude	magnitude
0	22.68	2.443	Residue Shape	0.00505895	0.00367955	0.00404956
1	29.04	1.336	Residue Shape	0.0097148	0.0191741	0.0208998

Chapter 3: System Identification

2	34.74	2.105	Residue Shape	0.0369463	0.0529193	0.0610965
3	40.05	2.784	Residue Shape	0.00242215	0.0179184	0.0215443
4	43.31	2.368	Residue Shape	0.019318	0.0981001	0.0874305
5	49.62	0.8021	Residue Shape	0.000749112	0.00222257	0.00218348
6	50.29	2.162	Residue Shape	0.00307012	0.0152884	0.0132733
7	45.78	-4.392	Residue Shape	0.0345218	0.106962	0.0508661
8	53.56	1.157	Residue Shape	0.0333832	0.0188864	0.0195637
9	58.2	1.331	Residue Shape	0.0906203	0.0617275	0.0450441
10	85.79	0.2307	Residue Shape	0.0001737	0.00150597	0.0054208
11	87.28	0.3554	Residue Shape	0.00584494	0.0242989	0.00429695
12	105.9	1.114	Residue Shape	0.000199115	0.0002198	0.0001596
13	124.7	0.3561	Residue Shape	0.0155728	0.00076488	0.0007754
14	130.8	-0.4139	Residue Shape	2.11E-06	3.45E-05	2.53E-05
15	147.6	0.6466	Residue Shape	0.000534169	0.00364881	0.0049906
16	154.3	0.5684	Residue Shape	0.00610854	0.013879	0.00212628
17	176.4	0.862	Residue Shape	0.00670819	0.0163996	0.0115843
18	179.2	0.3049	Residue Shape	0.00154019	0.00169844	0.0004933
19	189.4	0.5215	Residue Shape	0.00124655	0.0135343	0.00387029

Based on the table which is provided by the ModalVIEW software, the natural frequency, damping ratio and the magnitudes can be obtained. However, the magnitude is not included in the FRF but the mode shape. It is also required to calculate the mode shape from the information in the table 3.1.

Based on the equation 3.3.1 [32], the mode shape of each mode is obtained.

$$\varphi = M * 2\omega\sqrt{1 - \zeta^2} \quad (3.3.1)$$

, where ζ represents the damping ratio, M represents magnitude, φ represents the mode shape, and ω represents the natural frequency.

Then, in the ModalVIEW software, a Multidegrees of Freedom polynomial curve fitting function is used to estimate FRF parameters which are the natural frequency, damping ratio and mode shape, which is shown in the table 3.2.

Table 1.2 Modal parameters

Input from transducer 1			1Y : 1Y	2Y : 1Y	3Y : 1Y
Index	Frequency (Hz)	Damping (%)	φ	φ	φ
0	22.26	2.11	2.0531	1.7447	2.2110
1	27.84	1.924	14.1454	0.7454	2.4649

Chapter 3: System Identification

2	29.16	1.036	2.5484	2.8578	2.9036
3	34.79	1.866	9.9935	15.7963	18.6406
4	42.03	1.768	0.4608	1.6624	1.7801
5	43.77	1.842	1.3535	8.8618	7.8030
6	49.67	-0.008539	0.0239	0.0057	0.0001
7	53.7	1.047	45.6005	19.6973	22.1916
8	58.06	1.458	90.5574	63.5692	47.0703
9	85.62	0.2173	0.1326	0.7478	3.9263
10	124.7	0.3444	39.5723	1.9186	2.1134
11	147.2	0.5374	3.6184	7.9064	15.3631
12	148.2	1.534	10.0271	21.2950	24.3602
13	176.3	0.5288	10.6088	14.4058	14.3676
14	179.1	0.5678	36.0350	46.6070	7.1169
15	189.7	0.5049	0.1323	4.9308	1.5600
Input from transducer 2			1Y : 2Y	2Y : 2Y	3Y : 2Y
Index	Frequency (Hz)	Damping (%)	φ	φ	φ
0	22.36	2.33	1.4362	1.3305	1.3818
1	27.68	1.559	2.5301	0.4955	0.8598
2	29.01	1.489	4.2439	8.4493	9.1842
3	32.95	-0.4644	0.0165	0.0568	0.0460
4	34.72	2.612	22.3877	32.5810	37.8622
5	40.36	2.708	1.5652	11.6350	14.8044
6	43.01	2.635	11.3928	60.4619	53.8024
7	47.26	-1.242	0.1719	0.4827	0.1514
8	49.85	0.01635	0.0069	0.0075	0.0179
9	53.55	0.7323	21.1431	11.2754	11.7023
10	58.23	1.117	50.3913	34.7368	24.7710
11	85.69	0.243	1.0975	3.9374	23.0951
12	87.77	0.2926	0.4314	1.5733	0.7478
13	111.3	1.717	0.5296	0.5979	0.8488
14	124.6	0.3087	23.0652	0.9947	1.2397
15	147.4	0.763	1.6163	8.5468	13.1164
16	154.3	0.6028	7.3900	15.1288	2.3683
17	176.3	0.5722	10.7335	14.2664	14.7077
18	179.2	0.596	25.8537	33.2144	5.3835
19	189.3	0.4941	2.5571	29.4910	8.6146
Input from transducer 3			1Y : 3Y	2Y : 3Y	3Y : 3Y
Index	Frequency (Hz)	Damping (%)	φ	φ	φ
0	22.68	2.443	1.4414	1.0484	1.1538
1	29.04	1.336	3.5449	6.9965	7.6262
2	34.74	2.105	16.1255	23.0971	26.6661

Chapter 3: System Identification

3	40.05	2.784	1.2186	9.0145	10.8387
4	43.31	2.368	10.5109	53.3759	47.5706
5	49.62	0.8021	0.4671	1.3858	1.3614
6	50.29	2.162	1.9397	9.6594	8.3863
7	45.78	-4.392	19.8408	61.4746	29.2344
8	53.56	1.157	22.4672	12.7107	13.1665
9	58.2	1.331	66.2704	45.1412	32.9406
10	85.79	0.2307	0.1873	1.6235	5.8440
11	87.28	0.3554	6.4106	26.6507	4.7128
12	105.9	1.114	0.2650	0.2925	0.2124
13	124.7	0.3561	24.4028	1.1986	1.2152
14	130.8	-0.4139	0.0035	0.0566	0.0416
15	147.6	0.6466	0.9908	6.7677	9.2563
16	154.3	0.5684	11.8442	26.9108	4.1228
17	176.4	0.862	14.8695	36.3517	25.6780
18	179.2	0.3049	3.4683	3.8247	1.1109
19	189.4	0.5215	2.9668	32.2121	9.2114

Based on the information from the table 3.2, the fitting curves compared with measuring curves are shown in figure 3.3.2.

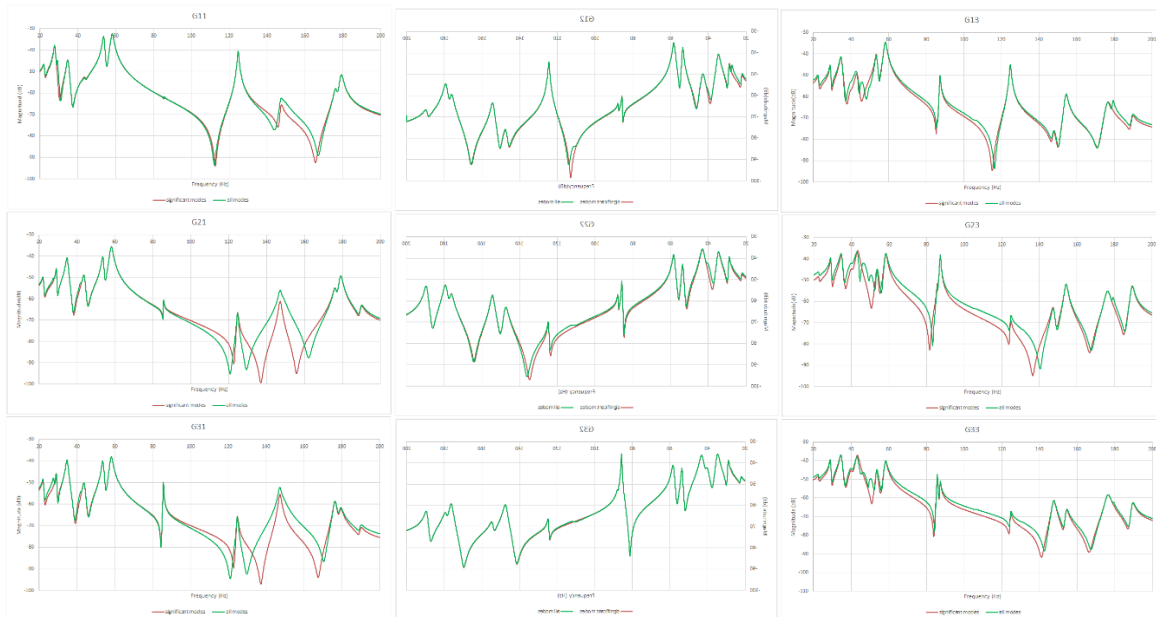


Figure 3.3.2 Comparison of FRF curves of all modes and significant modes

In the 3.3.2, the first column three curves refer to the signals input from transducer 1 and the second with the input from transducer 2 and so on.

Dynamics of flexible structure often consist of infinity number of modes, hence the influence from higher orders exists. However, with the purpose to control the first three modes of the plate, the residual function small enough to be ignored in current control purpose situation. With an aim to compare the optimization result with the unoptimized control system and other

optimized controllers, the parameters of the mathematical models are unified and simplified. The unified parameters of the structure is shown in table 3.3.

Table 2.3 Unified Modal parameters

	1 st Mode			2 nd Mode			3 rd Mode		
	F(Hz)	Dam- ping%	Mode shape	F(Hz)	Dam- ping	Mode shape	F(Hz)	Dam- ping	Mode shape
G11	22.66	2.667	0.132387	29.05	2.533	0.522717	34.86	2.419	0.20722
G12	22.66	2.667	0.092623	29.05	2.533	0.238071	34.86	2.419	0.386224
G13	22.66	2.667	0.07954	29.05	2.533	0.094088	34.86	2.419	0.336231
G21	22.66	2.667	0.117467	29.05	2.533	0.081823	34.86	2.419	0.36751
G22	22.66	2.667	0.079589	29.05	2.533	0.230657	34.86	2.419	0.70789
G23	22.66	2.667	0.063085	29.05	2.533	0.235156	34.86	2.419	0.588276
G31	22.66	2.667	0.098985	29.05	2.533	0.082337	34.86	2.419	0.321649
G32	22.66	2.667	0.042448	29.05	2.533	0.249072	34.86	2.419	0.609829
G33	22.66	2.667	0.056874	29.05	2.533	0.198524	34.86	2.419	0.574678

3.4 Differential Equation Derivation

With the aim to calculate the rang of the compensator's parameters which ensure the control system is occurred in stable condition, the frequency transfer functions are required derived into differential equation form.

The mathematical equation of frequency transfer functions is defined as equation (3.3.3) in the previous section. By simplifying the mathematical model of the plate, which is assuming the nature frequency and damping ratios are shared when the order of the mode is same, a decoupling operation is proposed, which divides system into 3 main parts, and each part is only related to one mode. There also exists 3 equations which are represented the relationship between inputs and decoupled outputs. The equation is shown in the equation (3.4.1).

$$y_i^n(s) = \sum_{j=1}^3 \frac{\varphi_{ij}^n u_j(s)}{s^2 + 2\zeta^n \omega^n s + \omega^{n^2}} \quad (3.4.1)$$

, Where $y_i^n(s)$ is the i^{th} output of the n^{th} mode, $u_j(s)$ represents the j^{th} input,

The output signals are represented in the equation (3.4.2)

$$\begin{bmatrix} y_1 \\ y_2 \\ y_3 \end{bmatrix} = \begin{bmatrix} y_1^1 + y_1^2 + y_1^3 \\ y_2^1 + y_2^2 + y_2^3 \\ y_3^1 + y_3^2 + y_3^3 \end{bmatrix} \quad (3.4.2)$$

Therefore, by combining equations (3.2.2) and (3.4.2), there are common parts in the transfer matrix for each mode, so the following definition can be made:

$$x_i(s) = \frac{\begin{bmatrix} \varphi_1^i \varphi_2^i \varphi_3^i \\ u_1(s) \\ u_2(s) \\ u_3(s) \end{bmatrix}}{s^2 + 2\zeta_i \omega_i s + \omega_i^2} \quad (3.4.3)$$

Where φ represents the eigenvector of the corresponding transducer position.

By taking inverse Laplace transform, the transfer function is translated into time domain from s-plane. The function is shown below.

$$\ddot{x}_i(t) + 2\zeta_i \omega_i \dot{x}_i(t) + \omega_i^2 x_i(t) = \begin{bmatrix} \varphi_1^i & \varphi_2^i & \varphi_3^i \end{bmatrix} \begin{bmatrix} u_1(t) \\ u_2(t) \\ u_3(t) \end{bmatrix} \quad (3.4.4)$$

Combine the equation (3.3.1) with equation (3.3.2).

$$\begin{bmatrix} Y_1^i(t) \\ Y_2^i(t) \\ Y_3^i(t) \end{bmatrix} = \begin{bmatrix} \varphi_1^i \\ \varphi_2^i \\ \varphi_3^i \end{bmatrix} x_i(t) \quad (3.4.5)$$

, where Y_1^i , Y_2^i and Y_3^i represent to the output signals obtained from the first, second and third transducer related to the i^{th} mode.

Then, by adding each decoupled output together, and rewriting the equation (3.4.3), the differential equations can be derived as equation (3.4.5) and equation (3.4.6).

$$\begin{bmatrix} \ddot{x}_1(t) \\ \ddot{x}_2(t) \\ \ddot{x}_3(t) \end{bmatrix} + 2 \begin{bmatrix} \zeta_1 \omega_1 & 0 & 0 \\ 0 & \zeta_2 \omega_2 & 0 \\ 0 & 0 & \zeta_3 \omega_3 \end{bmatrix} \begin{bmatrix} \dot{x}_1(t) \\ \dot{x}_2(t) \\ \dot{x}_3(t) \end{bmatrix} + \begin{bmatrix} \omega_1^2 & 0 & 0 \\ 0 & \omega_2^2 & 0 \\ 0 & 0 & \omega_3^2 \end{bmatrix} \begin{bmatrix} x_1(t) \\ x_2(t) \\ x_3(t) \end{bmatrix} = \begin{bmatrix} \varphi_1^1 & \varphi_2^1 & \varphi_3^1 \\ \varphi_1^2 & \varphi_2^2 & \varphi_3^2 \\ \varphi_1^3 & \varphi_2^3 & \varphi_3^3 \end{bmatrix} \begin{bmatrix} u_1(t) \\ u_2(t) \\ u_3(t) \end{bmatrix} \quad (3.4.5)$$

$$\begin{bmatrix} y_1(t) \\ y_2(t) \\ y_3(t) \end{bmatrix} = \begin{bmatrix} \varphi_1^1 & \varphi_1^2 & \varphi_1^3 \\ \varphi_2^1 & \varphi_2^2 & \varphi_2^3 \\ \varphi_3^1 & \varphi_3^2 & \varphi_3^3 \end{bmatrix} \begin{bmatrix} x_1(t) \\ x_2(t) \\ x_3(t) \end{bmatrix} \quad (3.4.6)$$

In this chapter, combining physical experimental modelling method and professional modal analysis software, ModalVIEW, the MIMO system is identified by following operations which are generating mathematical expression of the FRF, experimental modelling, FRF curves observing, measuring and fitting. The use of the ModalVIEW can estimate the FRF parameters, such as the natural frequency, damping ratios and the mode shapes. Then, with the purpose of design and optimizing the time-varying system, the system is identified in differential equation form.

Chapter 4 : Online Optimization Preparatory Work

With a purpose of optimizing an adaptive system online, some indispensable operations, such as the estimation of the time-varying structure and definition of target parameters, are performed before optimizing the adaptive control system. Since the online optimization requires a few computation times, a sub-optimization step is requested as well. In this chapter, the estimation of the structure strategy is designed firstly. Secondly, the selected controller, Positive Position Feedback(PPF) controller, is introduced, and the parameters of the controller is analyzed and preconditioned for online optimization. Finally, a sub-optimization approach is designed based on the Switching Multiple Model control theory.

4.1 Time-varying Structure Parameters Estimation

In this project, the time-varying system is designed as a varying loaded condition system. There are two exactly same loads to provide three kinds of loaded conditions. The fully loaded condition is proceeded when both loads loaded on the plate. With the aim to reduce all the influence but the weight, one load is set on the top of the other. The half-loaded condition is performed by setting one load and no load performs the unloaded condition.

According to the adaptive control theory, the parameters of controllers should be amenable when the object structure varies. Since design and optimization of vibration cancellation compensators of the system are required an accurate mathematical model of the system, the system estimation of time-varying structure takes a very important place. According to the structure of the mathematical model of the plate, parameters which are required to estimated are the nature frequencies, damping ratios and mode shapes. The aim of the control system is to cancel the effect from resonance, and a resonance occurs when the frequency of disturbance signal matches the natural frequency of the structure. According to this, the natural frequency is firstly estimated. Normally, the estimation of the natural frequency is performed via three approaches which are Zero-crossing method, Fast Fourier Transformation (FFT) and Recursive Least-Squares(RLS). Considering the computation time and the characteristic of this control system which is a MIMO system with Multi-mode vibration cancellation purpose, the FFT

method is selected in the natural frequency estimation [21]. Based on the estimated natural frequency of the plate, mode shapes will be figured out subsequently.

FFT is a fast algorithm of discrete Fourier transform. According the odd, even, imaginary and real characteristics of discrete Fourier transform to improve the algorithm of discrete Fourier transform. For a unknown disturbance signal which causes resonance, taking FFT operation can observe and analyze this signal on the frequency-domain. By ensuring the natural frequency band wide of each mode, taking an inverse FFT operation can obtain the natural frequency of the structure. The FFT and inverse FFT functions are provided by the Matlab software. After obtaining the natural frequency band of each mode from the experiments, the natural frequency can be estimated.

When the weight of the objects which are loaded on the structure the natural frequency and the mode shape have a decrement, but there exists a rising trend of the value of damping ration. For a flexible structure, there exists a linear relationship between natural frequency and corresponding mode shape. Therefore, the estimated natural frequencies can be used to figure out the mode shapes. when there is a variation loaded condition of the structure, the structure can be considered as a Mass-Stiffness-Damp system [34]. The dynamic response function of plate can be written as:

$$\Delta h(t) = A_m e^{-\zeta \omega_n t} \sin(\omega_d t) \quad (4.1.1)$$

,where A_m is the maximum amplitude; ζ is the damping radio of the structure; ω_n is the damped natural frequency; ω_d is the non-damped natural frequency.

The expressions of vibration dynamic performance index of the structure are:

$$A_m = \frac{1}{\alpha M \omega_d} \quad (4.1.2)$$

$$\omega_d = \omega_n \sqrt{1 - \zeta^2} \quad (4.1.3)$$

$$\omega_n = \sqrt{\frac{K_\alpha}{\alpha M}} \quad (4.1.4)$$

$$\zeta = \frac{C_\alpha}{2\sqrt{\alpha MK_\alpha}} \quad (4.1.5)$$

, where α represents the coefficient of the mass, M represents the mass of the plate in fully loaded condition; C_α represents the damp of the structure, and K_α represents the stiffness.

Obviously, the vibration dynamic performance indexes are all related to the basic performance parameters of the structure. However, in the actual operations, these parameters cannot be obtained directly and quickly. With the purpose of estimating the vibration indexes in a specific loaded condition, all of the indexes are required to be identified in the initial condition. Then, by estimating natural frequency in current condition and comparing it with initial natural frequency value, the variational coefficient can be ensured. Combine equation (4.1.2) with equation (4.1.3) and equation (4.1.4). The relationship between natural frequency and maximal amplitude is shown in the equation (4.1.6).

$$\frac{A_m}{\omega_n} = \frac{1}{K_\alpha \sqrt{1-\zeta^2}} \quad (4.1.6)$$

Due to the fact that damping ratio of this plate is very small that the order of magnitude of it is 10^{-2} , the value of $\sqrt{1-\zeta^2}$ can be set as a constant. By assuming the stiffness is stable, the maximal amplitude and natural frequency will share a same variational coefficient. The expression of maximal amplitude estimation is:

$$A_m = A_{mi} \frac{\omega_n}{\omega_{ni}} \quad (4.1.7)$$

, where A_m represents the current maximal amplitude; ω_n represents the current natural frequency; A_{mi} represents the initial value of maximal amplitude; ω_{ni} represents the initial value of natural frequency.

According to the modal analyzing theory [4], the expression of mode shape φ calculation is:

$$\varphi = A_m \omega_n \sqrt{1-\zeta^2} \quad (4.1.8)$$

And for the damping ratio, it is selected as the initial value because it has a very low order of magnitude and it is mainly related to the value of the structure's damp which is difficult to obtained.

After filling the transfer functions of the plate with estimated parameters, the estimation of the structure is finalized, so that the corresponding compensators are able to design and optimized.

4.2 Positive Position Feedback(PPF) controller

Due to a high robustness characteristic, PPF controllers have a well performance on time-varying structure control. Hence, the PPF controller is selected in this project. The basic principle PPF controller is to add extra damping to the target modes of the structure with the purpose of reducing the effect of the disturbance. In this section, the structure of the PPF controller is provided first, followed by the analyzation of parameters of the controller. Finally, the pretreatment of each parameter is constructed.

4.2.1 PPF controller structure

The PPF controller is constituted by three parameters, control frequencies, control damping ratios and control gains. In a SISO situation, the mathematical transfer function of PPF for the first three modes compensation purpose is

$$G_n(s) = \sum_{n=1}^3 \frac{\omega_{cn}^2}{s^2 + 2\zeta_{cn}\omega_{cn}s + \omega_{cn}^2} \quad (4.2.1)$$

, where n is the order the mode, ω_c represents the control frequency of the ζ_c represents the control damping ratio.

By taking inverse Laplace transform, equation (4.1.2) is transduced from frequency domain to time domain and combined with the equation (3.3.5) and equation (3.3.6), PPF controller system can be represented as:

$$\text{Structure: } \ddot{\xi} + 2\zeta\omega\xi + \omega^2\xi = g\omega^2\eta \quad (4.2.2)$$

$$\text{Controller: } \ddot{\eta} + 2\zeta_c\omega_c\dot{\eta} + \omega_c^2\eta = \omega_c^2\xi \quad (4.2.3)$$

, where ξ refers structure coordinate, ζ refers damping ratio of structure, ω refers natural frequency of structure, η refers compensator coordinate, ζ_c refers compensator damping ratios, ω_c refers compensator frequency and g refers compensation gain

The block diagram of PPF control system is shown in the Figure 4.2.1.

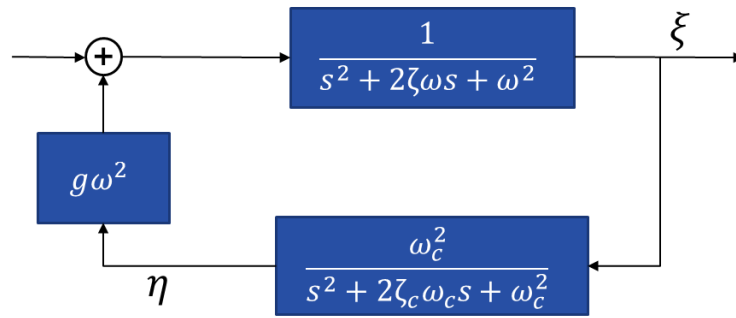


Figure 4.2.1 Block diagram of PPF control system

In the project, the control system is a MIMO system. According to the PPF control theory, the block diagram of multi-mode MIMO PPF control closed-loop system is shown in the Figure 4.2.2[35].

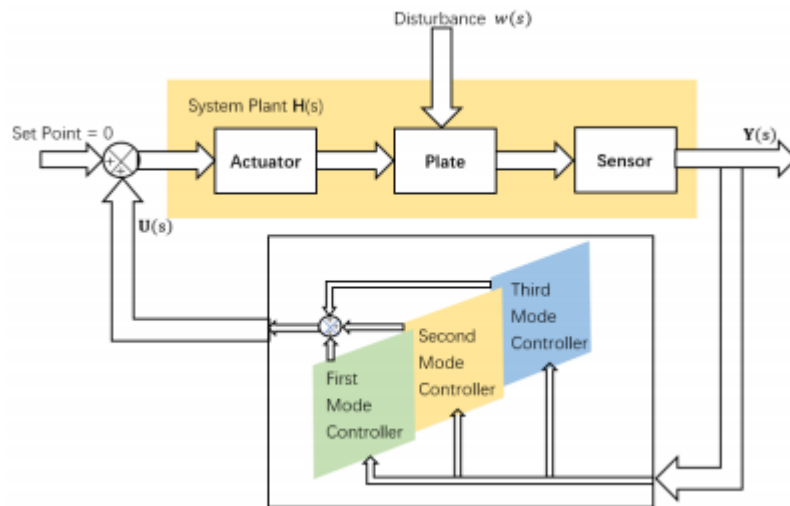


Figure 4.2.2. Block diagram of multi-mode MIMO PPF control closed-loop system [35]

According to the equations (4.2.2) and (4.2.3), the MIMO PPF control system can be represented as equations (4.2.4) and (4.2.5)

$$\text{Structure: } \ddot{X}(t) + \Psi \dot{X}(t) + W^2 X(t) = C_i W_c G Z(t) \quad (4.2.4)$$

$$\text{Controller: } \ddot{Z}(t) + \Psi_c \dot{Z}(t) + W_c^2 Z(t) = W_c C_o X(t) \quad (4.2.5)$$

$$W - C_i G C_o > 0 \quad (4.2.4)$$

Hence, each element in the gain matrix is from 0 to 1. With required range, gains are optimized in the followed chapters. With purpose of compensating the first three modes, there are three controller gains are requested to be optimized. In order to simplify the optimization operation, only one controller gain is optimized online at same time. Considering possible spill-over effect that high frequencies may introduce to low frequencies, the controller gain for the third mode of concern is optimized first, followed by the gains of the subsequent lower modes of concern.

4.3 Sub-optimization step design

Traditionally, the optimization of the system requires large amounts of computation time, and the system may become unstable until the optimization of the parameters completes [35]. Hence, it is not acceptable for a time-varying system. With the purpose of stabilizing the plate and providing enough computation time of further optimization operation, a sub-optimization step is performed.

In this section, according to the Switching Multiple Model(SSM) control theory, two provided controllers in unloaded condition and fully loaded condition are selected to constitute the core of the sub-optimization operation.

As a kind of adaptive control system, the block diagram of SSM control system is shown in the Figure 4.3.1.

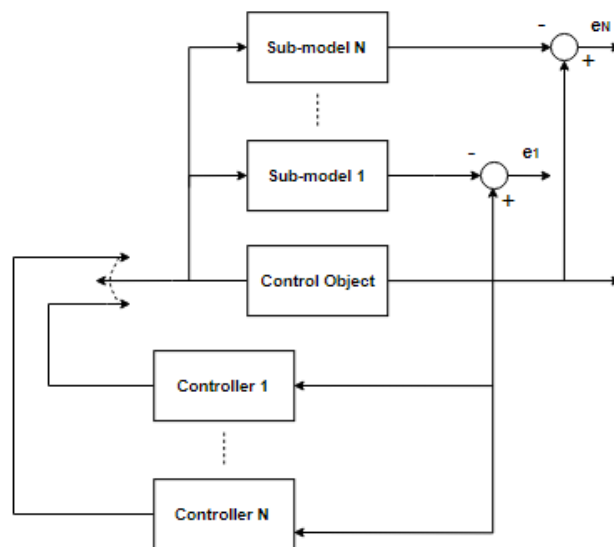


Figure 4.3.1 Block diagram of SSM control system

Chapter 4: Online Optimization Preparatory Work

In the traditional SSM control system, the control object is a time-varying structure [35]. By obtaining the minimal error between sub-models and the control object, the closest sub-model is ensured, and the corresponding controller is selected [37].

Since the controller in the sub-optimization step is used to temporarily control the structure, the high control performance demand is not required. Therefore, the number of the sub-models is two. These two sub-models are the mathematical models of the plate in the unloaded and fully loaded conditions as the plate in these two conditions can be modeled accurately and easily in experimental practice. Since the time-varying structure is caused by dynamically loaded condition and the varying natural frequency is a function of the loaded condition, the estimated natural frequency is used as the criterion of selection rather than by obtaining all the errors of the sub-models. This simplified operation can improve the response speed. According to the distribution of the teamwork, the PPF controllers in half-loaded and fully loaded conditions are designed and optimized off-line by the teammate, Yihao.

Chapter 5 : Online Optimization via Genetic Algorithm Approach

In Chapter 4, the natural frequency is provided by a frequency estimator designed by another project. As the discussion in the chapter 4, control frequency and the damping ratio of the PPF controller can be defined and selected based on the estimated natural frequency, hence only the controller gain is required to be optimized online via extra operation. As one of the most common optimization approaches, the Genetic Algorithm(GA) enables the operators to obtain the global solution in a higher change. In this chapter, the GA optimization theory is discussed. Then each procedure of the GA is designed and simplified for saving the computation time. Finally, a SISO single-mode PPF control system is performed to validate the GA approach.

5.1 Genetic Algorithm Theory

The Genetic Algorithm (GA) is a probabilistic optimization method developed by Professor JH Holland in the mid-1970s through the simulation of the biological evolution process [24]. It is a global optimization method based on natural selection principles and natural genetic mechanisms which aims at simulating the evolution natural life. GA has been widely used because it can effectively solve combinatorial and real-parameter optimization problems as well as complex function optimization problems. Comparing with GA, the conventional optimization methods are difficult to solve above problems. Moreover, GA has many advantages that it has a simple calculation process, has wide adaptability to the search space and no differentiability requirements for the function itself; hence, GA is especially suitable for dealing with complex control optimization problems [15].

Traditionally, GA is consisted of steps shown in the Figure 5.1. Firstly, initialization is proceeded. In this step, a population with parameter coding is generated as the first generation. The next step is evaluating the fitness of each individuals. Subsequently, by checking the order of current generations and the highest fitness value, a decision is made to either return the best solution or generate a new population. If the number of the generation meets the maxim number of generations or the highest fitness meets criteria, the best solution is returned followed by parameter decoding operation. Otherwise, a new generation is proceeded. Thirdly, the selection step is processed to select the individuals from the population to carry out following steps,

Crossover and Mutation. Finally, new individuals are placed into the population and go back to the second step.

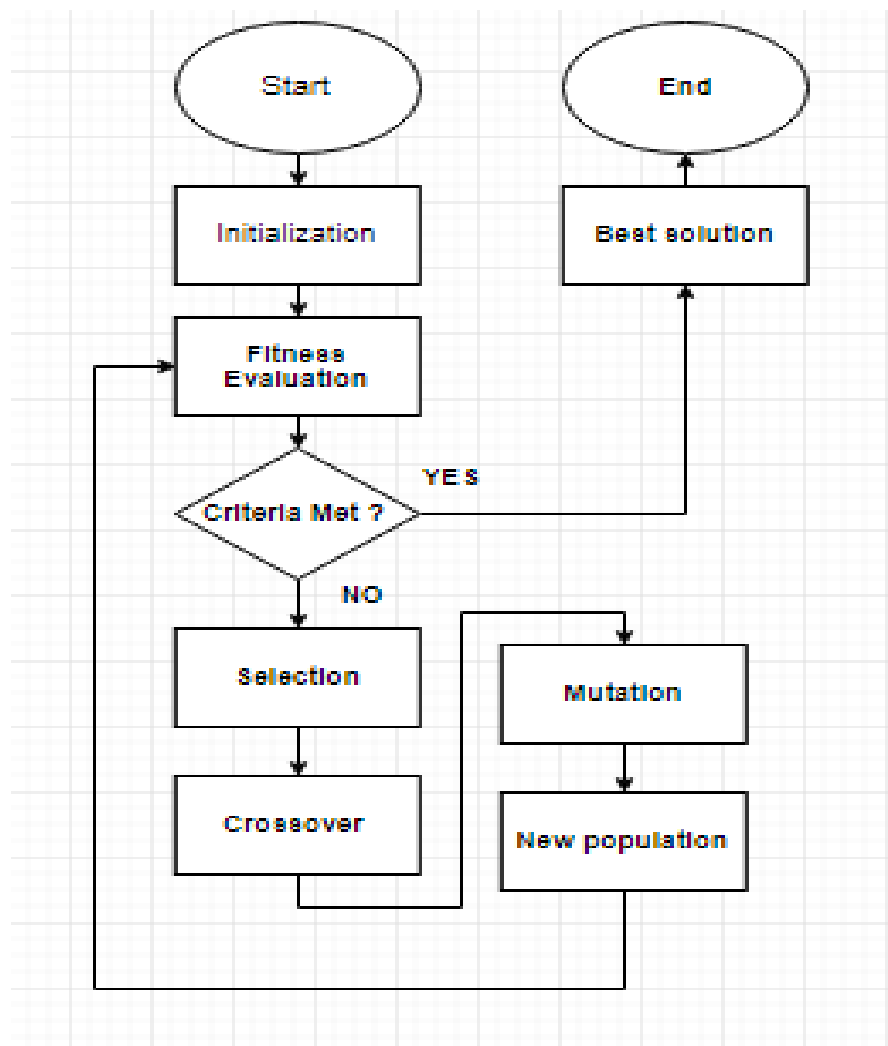


Figure 5.1 Block diagram of GA

In initialization, selection, crossover and mutation steps of GA, there also exists several strategies to be proceeded.

5.2 Genetic Algorithm Online Optimization Design

By discussing the advantages and shortcomings of these strategies and considering the characteristics of the selected control system and online optimization purpose, the most suitable strategy of each step is selected.

5.2.1 Initialization

In the initialization step, there are two common parameter coding schemes, binary coding and real-number coding, for one-dimensional problems.

Binary coding uses binary coded symbol set $\{0,1\}$, and each individual designed as a sequence, which is called chromosome in GA. According to the model theory, the binary coding scheme is most widely employed, and almost every problem can be expressed in binary coding. Therefore, binary coding method applications is the earliest and most extensive, which is the most common encoding scheme in GA [16].

Obviously, the major advantages of the binary encoding scheme are:

- a) The encoding and decoding operations are simple and easy;
- b) Genetic manipulations such as selection, crossover and mutation are easy to put into practice implement;
- c) Binary coding complies with the minimum symbol set encoding principle;
- d) Facilitate the use of pattern theorem to theoretically analyze the algorithm.

However, when binary coding scheme deals with multi-dimensional and high-precision continuous function optimization problems, there are major shortcomings of the binary coding scheme as follow:

- a) Binary coding sometimes does not reflect inherent structural features and specific information (e.g., position and direction). in other words, it is difficult to directly describe the qualities of the problem, which makes it inconvenient to design genetic operators for specific problems.
- b) The use of binary coding requires frequent encoding and decoding, which will increase both the computational complexity of the algorithm and the numbers of conversion error and may cause premature convergence of the algorithm. The efficiency of the algorithm drops sharply with the increase of both variables and calculation accuracy.

The second common scheme is real-number coding. In this scheme, each individual's chromosome is constituted by a set of real numbers (or floating-point numbers) in a certain range. The size of the set equals to how many variables are required to be computed in fitness evaluation. Compared with binary coding, real-number coding is directly encoded in the form

of solution space. This means genetic operations do not need frequent encoding and decoding and the length of the chromosome can be greatly shortened. Therefore, the computational complexity of GA and the efficiency of the algorithm are improved. Moreover, specific information is easy to represent in a specific field by using real-number coding scheme.

Nevertheless, real-number coding is not based on the pattern theorem. Its crossover and mutation operations are just forms. Therefore, its global search ability is weaker compared with binary coding and the gene manipulation is not flexible enough.

In this project, the compensator parameters that needs to be optimized is the gain matrix only. The range of each gain is from 0 to 1 and elements of gain matrix is optimized respectively. Hence, there is only one value is required to optimize in each GA computation loop. According to this, the binary coding scheme is selected in the initialization step. With the purpose of randomly selecting the first generation, population is represented by a matrix of i rows and j columns. i is the size of the population and j is the length of each individual's chromosome. And each elements of this matrix selected as 0 or 1 randomly. As a result, the first-generation population is generated and encoded, then each individual will be evaluated its fitness in the next step. The population size is designed as minimal requirement which is 20 aims to save the computation time [7]. According to the required accuracy (accurate to 0.0001) of gain, j is designed as 14 since $2^{-14} = 0.000061$ as an element consists the parameters.

5.2.2 Fitness Evaluation

In this operation, all of individuals are required to compute their fitness. Based on the fitness of each individual, individuals will be sorted from high fitness to low fitness. In order to evaluate the fitness of each individual, the evaluation function is required to be selected and designed. H_2 norm theory and H_∞ norm theory is always used to compute the control performance in the vibration control system [27].

From the viewpoint of vibration control, the value of H_2 norm reflects the power in the entire frequency band of the system. Therefore, by using H_2 norm theory to optimize, the sum of the squares of all the singular values of the system is suppressed, or all the formants of the vibration system are suppressed at the same time. Optimizing by using H_∞ norm theory is to minimize the maximum singular value of the system, i.e., the maximum gain of the system transfer function on the respective input direction over the entire band.

Compared with H_2 norm theory, H_∞ norm theory is particularly suitable for dealing with control optimization of multiple-input multiple-output systems. Moreover, due to the influence of residual modal, parametric perturbations and the presence of errors in the sensor and actuator systems model, the accurate control model is difficult to be established [6]. H_∞ norm theory can handle the robust performance problems and robust stability of linear systems well. Hence, the fitness of each individual is ensured by computing the value of H_∞ of the control system.

In order to calculate the value of H_∞ , the closed-loop transfer function matrix is required. With already estimated structure mathematical model of the plate and filled compensators' transfer functions with parameters which are the individuals in GA, the value H_∞ of can be calculated by using MATLAB. Due to the fact that lower H_∞ means that the compensators provide more effective compensation, the fitness value of each individual is designed as the reciprocal of H_∞ value of corresponding closed-loop transfer function matrix.

5.2.3 Selection

Selection operation is applied to achieve survival of the fittest in individuals of the group. This means that Individuals with high fitness are more likely to be inherited into the next generation; individuals with lower fitness have small probability to be inherited into the next generation. Roulette wheel selection, also known as proportional selection method, is proceeded as selection operation. The basic idea is that the probability of each individual being selected is directly proportional to its fitness. The specific operation is proceeded as below.

- (1) Calculate the fitness of each individual in the population, which has been done in the operation
- (2) Calculate the probability of each individual would being inherited into the next generation;
- (3) Calculate the cumulative probability of each individual, which is represented by P1, P2, P3...Pn (n is the size of the population);
- (4) Generate a uniformly distributed pseudo-random number r in the [0,1] interval;
- (5) If r is less than P1, select first individual; otherwise, select the individual, which meets the condition:

$$P_{i-1} < r \leq P_i \quad (5.2.1)$$

Then a population which is constituted by selected individuals is required to sorted by the fitness again. This aims at processing subsequent crossover and mutation operations.

5.2.4 Crossover and Mutation

The crossover operation indicates the exchange of some genes between two mutually matched chromosomes in a certain way, thereby forming two new individuals. The mutation operation refers to replacing certain gene values in individual code strings with other gene values to form a new individual. The mutation operation in the GA is an auxiliary method to generate a new individual. However, the mutation operation is indispensable because it determines the search capability of the GA. The mutual cooperation of the crossover operation and the mutation operation completes the global search. As important features of GA, crossover and mutation operations distinguish GA from other evolutionary algorithms. These two operations are the main methods for generating new individuals.

However, traditional crossover and mutation operations may cause premature convergence. In order to overcome this shortcoming and improve GA global exploration ability, an Adaptive genetic algorithm (AGA) method is proposed to determinate Probability of Performing Crosser (Pc) and Probability of Mutation (Pm) [17]. Individuals fitness higher than the average fitness of the population correspond to lower Pc and Pm, so that the solution is protected into the next generation. Individuals with lower fitness than the average fitness of the population correspond to higher Pc and Pm, as a result, the solution is eliminated. Therefore, AGA can provide the best Pc and Pm for a certain solution, which ensures the diversity of the population in the evolutionary process and the minimal number of generations can be reduced with the aim to lead the search to the global optimum.

According the theory of AGA, the Pc and Pm are designed respectively.

$$p_c = \begin{cases} p_{c1} - \frac{(p_{c1} - p_{c2})(f' - f_{avg})}{f_{max} - f_{avg}} & f' \geq f_{avg} \\ p_{c1} & f' < f_{avg} \end{cases} \quad (5.2.2)$$

$$p_m = \begin{cases} p_{m1} - \frac{(p_{m1} - p_{m2})(f - f_{avg})}{f_{max} - f_{avg}} & f \geq f_{avg} \\ p_{m1} & f < f_{avg} \end{cases} \quad (5.2.3)$$

, where f_{\max} is the largest fitness value in the population, f_{avg} is the average fitness value of the population; f' is to cross the more considerable fitness value in two individuals; f is the fitness value of the individual to be mutated. Different sets of probabilities of Performing Crossover from 0.5 to 0.95 at an incremental step of 0.05 are tested for each step. The most suitable Performing Crossover is found when $p_{c1} = 0.9$ and $p_{c2} = 0.6$. In terms of Pm, the test is performed in its normal range, 0 to 0.2, increased by 0.01 for each step. Based on the results of the test, the value of Pm is set to be $p_{m1} = 0.1$ and $p_{m2} = 0.01$ [17].

After processing crossover and mutation operations, a new population has been generated. This new-generation group will replace the previous-generation group. Then the fitness evaluation operation will be proceeded again until the maxim number of generations is achieved. According the article [17] and the accuracy requirement of this project, the maxim number of generation can be reduced to 20 by applying this crossover and mutation strategies.

5.2.5 Decoding

When evaluate fitness and return best solution, the individuals are required to process decoding operation Due to the fact that binary coding scheme is selected in the initialization operation, the individuals are decoded based on the equation (5.2.4). After decoding the chromosome, each individual is represented in real-number space in the range of the compensator parameter.

$$x = b_{\text{low}} + \sum_{i=1}^l b^i * 2^{i-1} \frac{(b_{\text{high}} - b_{\text{low}})}{2^l - 1} \quad (5.2.4)$$

, where l is the length of the binary chromosome, b_{low} is the lower bound of x , b_{high} is the higher bound of x , b^i is the value of chromosome at the i th position.

Overall, although the genetic algorithm is a random search algorithm, GA can explore a new generation of individuals with good fitness. The new-generation population are obtained by the initial population through selection, adaptive crossover and adaptive mutation operations. By performing the fitness evaluation operations of each individual, the further operation is decided. If the end condition is satisfied, the best solution is returned. Otherwise, the above operations are required to repeat. After repeated iterations like this, the global optimal solution can be obtained in the end.

5.3 Simulation Construction and Explanation

In this section, a SISO single-mode system is generated via the MATLAB SIMULINK in order to validate GA approach. The model of this control system is shown in the Figure 5.3.1. In this model, the plate is already estimated and the optimized controller in unloaded condition is selected as the sub-controller. The optimization operation is performed and timed via the MATLAB. The MATLAB script can refer to Appendix A. The compare between the uncompensated and compensated by pre-designed compensator system responses is first obtained. After optimizing the gain and generating the optimized the controller, the compare between the uncompensated and compensated by the optimized compensator system responses is subsequently obtained.

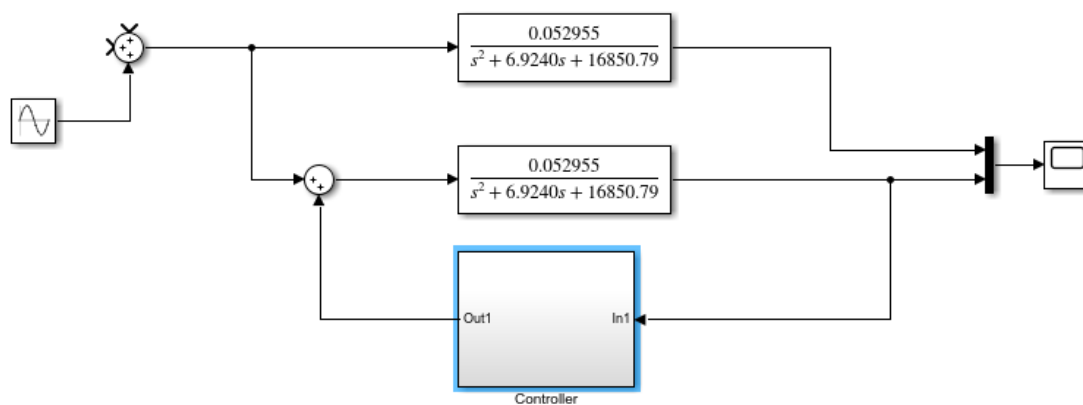


Figure 5.3.1 Block diagram of the SISO single-mode control system

The subsystem of the controller is shown in the Figure 5.3.2.

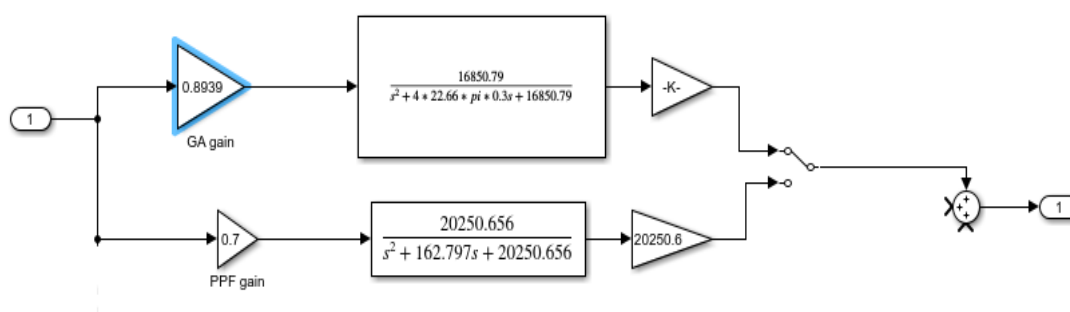
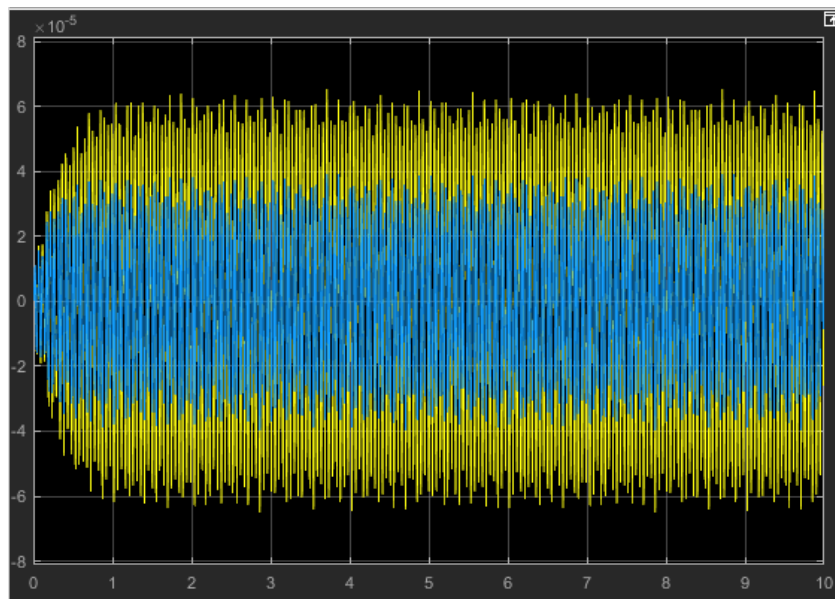
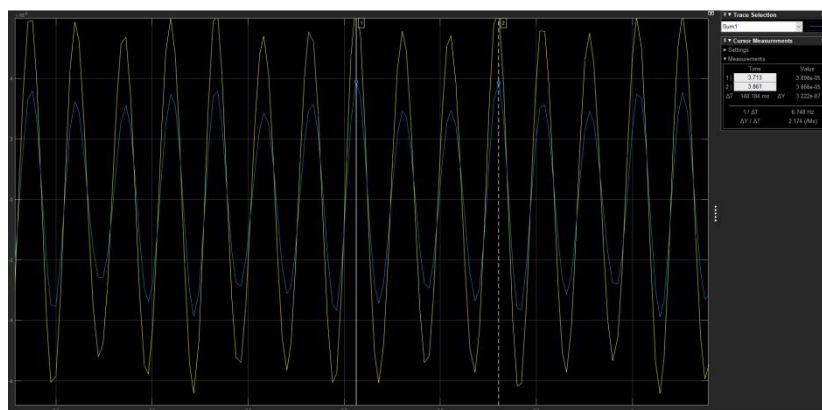


Figure 5.3.2 Block diagram of the subsystem of controller

The compare of systems which are uncompensated and compensated by the per-designed controller is shown in the Figure 5.3.3.



(a)



(b)

Figure 5.3.3 Responses of the original and pre-designed controller control system

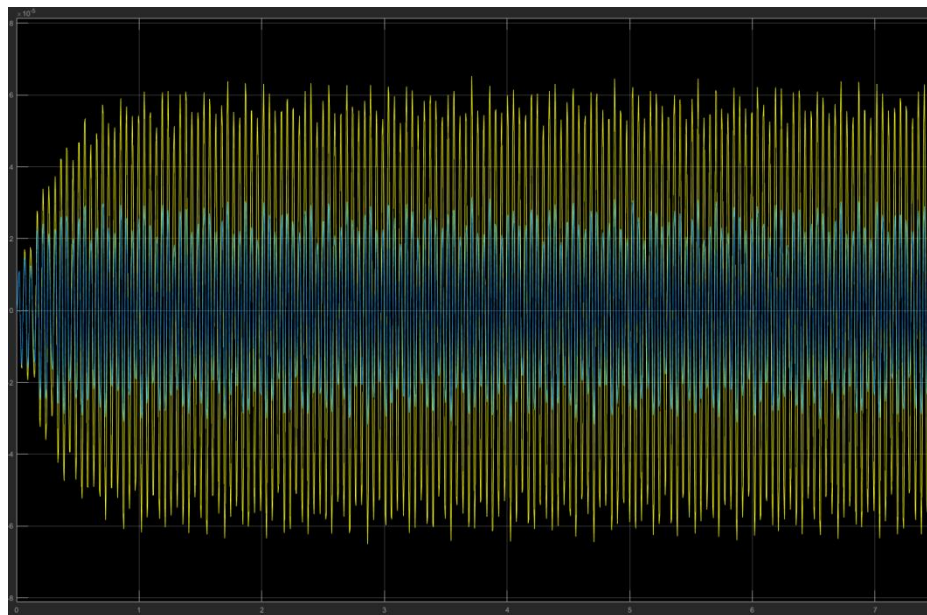
In the Figure 5.3.3(a), the plot refers to the responses of original system and compensated system. And the Figure 5.3.3(b) is the zoomed out and scaled version.

By using the MATLAB software, the gain of the new controller is optimized, the time of the computation is show in the Figure 5.3.4.

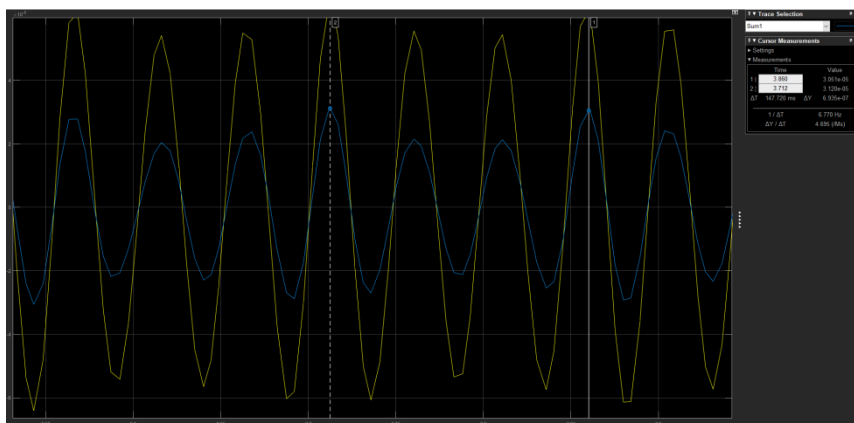
Function Name	Calls	Total Time	Self Time*	Total Time Plot (dark band = self time)
GASSSM	1	5.464 s	1.175 s	
normssf	200	4.288 s	0.034 s	

Figure 5.3.4 Computation time of the GA optimization operation

After optimizing the gain of the corresponding controller, the new optimized controller is switched on to replace the pre-designed controller. The compare between the uncompensated and compensated by the new optimized controller systems is shown in the Figure 5.3.5.



(a)



(b)

Figure 5.3.5 Responses of the original and optimized controller control system

In the Figure 5.3.5(a), the plot refers to the responses of original system and compensated system. And the Figure 5.3.5(b) is the zoomed out and scaled version.

For Figure 5.3.3, the yellow line refers to the response of the open-loop system in an unknown loading condition and the blue line refers to the response of system controlled by the pre-designed controller corresponding to unloaded working condition. For Figure 5.3.5, the blue line represents the response of the system with online optimized PPF controller. The magnitudes of the blue lines in these two figures are recorded and compared in Table 5.1 to validate the performance of the GA optimization approach.

Table 5.1 Control performance SISO single-mode control system optimized via GA

Controller	Attenuation
Predesigned controller	4.37 dB
Optimized adaptive controller	6.7dB

Chapter 5: Online Optimization via Genetic Algorithm Approach

According to the Table 5.1, a further 2.33 dB attenuation, around one third control performance improvement, can be achieved by using the optimized adaptive controller.

In conclusion, the adaptive controller that is optimized by GA approach can effectively improve the control performance. And for a simple control system, the computation time, 5.464 seconds, is acceptable.

Chapter 6 : Online Optimization via Simulated Annealing approach

Simulated Annealing (SA) algorithm is a general-purpose random search algorithm, which is an extension of the local search algorithm. Unlike general local search algorithms (e.g. Mountain Climbing algorithms), the SA approach can be performed to select a relatively small target value in the neighborhood with a certain probability. Therefore, the SA approach is a theoretical global optimal algorithm. In this chapter, the major elements of SA are first discussed and analyzed, followed by the design and simplification for the procedures of SA. Finally, a SISO single-mode control system which is required optimization is created to validate SA optimization approach.

6.1 Simulated Annealing Optimization Theory

The idea of simulated annealing was first proposed by Metropolis [19] in 1953. It originated from the study of statistical thermodynamic phenomena in the cooling process of objects. Kirkpatrick formally proposed the simulated annealing algorithm in 1982 and successfully applied it to combinatorial optimization problems. The basic idea of simulated annealing is to introduce a random disturbance to the deterministic algorithm so that the algorithm process has a small probability of “jumping” the local extremum trap when the survey point reaches the local extremum. The introduction of the Metropolis criterion in the combinatorial optimization process results in a combinatorial optimization algorithm that iterates the Metropolis algorithm. The SA algorithm is a heuristic stochastic optimization algorithm that simulates the physical annealing process. Starting from a given initial high temperature, a sampling strategy with probabilistic jump characteristics is used to search randomly in the solution space. The sampling process is repeated with decreasing temperature. Finally the global optimal solution of the problem is obtained. The characteristics of easy realization and global progressive convergence is widely used to solve some optimization problems in control system.

The SA algorithm major constituent elements are State expression, Neighborhood definition and movement, Thermal equilibrium condition and Cooling control.

6.1.1 State expression

State expression uses a mathematical form to describe the energy state of the system [18]. State expression is the basic work of SA and directly determines the construction and size of the

neighborhood. A reasonable state expression method will greatly reduce the computational complexity and improve the performance of the algorithm.

In SA, a state is a solution to the problem. The objective function of the problem corresponds to the energy function of the state. Three common state expression methods are

Binary coding which representations suitable for knapsack problem and assignment problem.

Natural-number coding that representations for scheduling problems

Real-number coding that representations suitable for various continuous function optimization.

With the aim of optimizing the parameters of compensator, the real-number coding is the most suitable state expression method. And because there is no required decoding operation, the computation time can be reduced.

6.1.2 Neighborhood definition and movement

Neighborhood is the value range of the next solution. The starting point of the definition of the neighborhood should meet the condition that the solution can be spread over the entire solution space as much as possible. The definition of the neighborhood is usually determined by the nature of the problem. In the optimization problem, by defining the step size, the domain of solution space, and the selection method of the new solution, the neighborhood will be defined. Next, the movement method from the current solution to a new solution is required to determine in its neighborhood. In the SA algorithm, a special Metropolis criterion is used for the neighborhood mobility method, i.e., according to a certain probability to determine whether the current solution move to the new solution.

The neighborhood movement in SA is divided into two modes: unconditional movement and conditional movement. If the value of the objective function of the new solution is less than the value of the objective function of the current solution (the energy of the new state is less than the energy of the current state), the unconditional movement is performed.

According to Metropolis criterion, the formula of the certain probability calculation is defined as:

$$P = \exp\left(\frac{|\Delta f|}{Tk}\right) \quad (6.3.1)$$

Δf - the difference value between the value of objective function of current solution and the value of objective function of new solution

Tk - current temperature

Then, comparing the probability to a random number in a range from 0 to 1, if the probability is greater, the new solution is accepted and replace the current solution. Otherwise, the new solution rejected. And the thermal equilibrium condition estimation operation is performed.

As a key factor to achieve SA global search, this neighborhood mobility method can ensure that the algorithm has the ability to jump out of the local minimum to global optimization. When the temperature is very large, the certain probability tends to 1, and the SA performs wide area search, which means it will accept any solution in the current neighborhood even if the solution is worse than the current solution. And when the temperature becomes very small, the probability tends to 0; therefore, the SA is performing a local search, i.e., it will only accept the better current solution in the neighborhood.

6.1.3 Thermal equilibrium condition

The achievement of thermal equilibrium is equivalent to the isothermal process in physical annealing, which refers to the process of SA performing a random search. The search is based on the Metropolis criterion at a given constant temperature, and finally reaching a state of equilibrium.

This is the internal loop process in the SA algorithm to ensure equilibrium, the number of internal loops is large enough. The most common method is to set the internal loop number to a constant. At each temperature, the loop iterates the same number of times. The selection of the number is related to the actual size of the problem. And this number is usually obtained based on some empirical formulas. Other method for setting the number of internal loops is based on the current temperature. When the temperature is high, there are fewer internal loops. while the temperature is decreasing, the number of internal loops increases.

6.1.4 Cooling control

As the outer loop process in the SA algorithm, the cooling control is proceeded based on a cooling function which is used to control the temperature drop mode. The core feature of SA is to use temperature drop to control the iteration. Theoretical, the SA only requires the temperature to eventually go to 0; therefore, there is no limit to set the rate of temperature drop. However, in actual operations, it does not mean that it is free to drop the temperature.

The temperature determines whether SA performs a wide area search or a local area search. If the temperature drops too quickly, SA will soon switch from wide area search to local search, which is likely to lead to prematurely falling into a local optimal state. In order to jump from the local optimization, it can only be achieved by increasing the number of inner loops, which

will greatly increase the arithmetic operation time. If the temperature drops too slowly, although the team can reduce the number of inner loops, the computation time will also be affected by the increase in the number of outer loops. Therefore, selecting a suitable rate of temperature drop and cooling function can improve the performance of the SA algorithm.

For providing a acceptable cooling control, there are two common cooling functions:

$$T_{k+1} = r \cdot T_k \quad (6.3.2)$$

, where $r \in (0.95, 0.99)$

$$T_k = \frac{T_0}{1+t(k)} \quad (6.3.3)$$

T_{k+1} - the temperature of next iteration

T_k - the temperature of current iteration

r - the rate of temperature drop

T_0 - the initial temperature

$t(k)$ -the start time of current iteration

To optimize the parameters of compensator online, the equation (6.3.2) is selected. It aims at reducing the computation time and improving the performance of the optimizer. Since the calculation and storage operations of the current time are not required in the equation (6.3.2), the speed of cooling operation is easily to reduce.

6.2 Simulated Annealing Procedures Design

For the optimization problem, obtaining minimal objective function $f(i)$ where $i \in S$ (i is the compensator's parameter which is required to optimize, and S is the domain of the parameter in discrete space), according to the theory of the SA algorithm, the calculation procedure of the SA algorithm is shown in the figure 6.3.1.

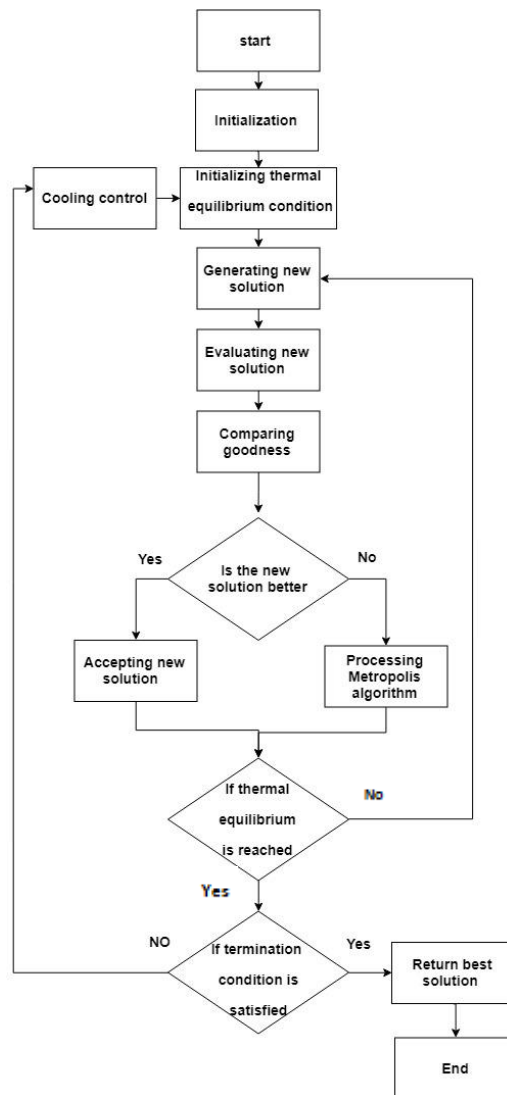


Figure 6.2.1 Block diagram of SA algorithm

In the initialization operation, initial and termination temperatures, initial value of the parameter and rate of cooling function are defined. Normally, the initial parameter is selected randomly in its range. In order to reduce the searching time, the initial value of gain is defined as the selected pre-designed controller.

The choice of initial temperatures also brings a large effect to the performance of the SA algorithm. The initial temperature should be large enough. According to the equation (6.3.4), the initial temperature is defined, which aims at ensuring that the algorithm has enough time to obtain the optimal solution. The termination temperature is defined as small as 1. The cooling rate is selected as 0.9, which is the minimal value in its traditional range.

Then the condition of the thermal equilibrium is initialized to ensure the inner loops can start with a brand-new condition. The condition the thermal equilibrium. After initializing the thermal equilibrium, the objective value of the new solution is calculated by using the objective function.

Similar to the GA, the objective function is selected for calculating the H_∞ value of the system. With the already calculated value of H_∞ , the goodness level of the solution is figured out. The relationship between the goodness and objective value is defined as that the smaller the H_∞ is, the better the solution is.

In order to furtherly obtain the general best solution. The comparing operation is modified as that the goodness of the new solution is not only compared with last solution's but also the best solution's in previous operations. And if the new solution is better, the best solution is replaced by the new solution and stored.

Then, the decision of whether new solution is accepted or not is made. The new solution will not be accepted if it is worse than the last solution and Metropolis criterion is not met.

Subsequently, by checking the number of inner loops which have been proposed, whether stopping inner loops or not will be determined.

Finally, the value of current temperature is compared with termination temperature. If the current temperature does not reduce to the termination temperature, the cooling operation is performed. And a new outer loop is switched on. Otherwise, the best solution is returned.

6.3 Simulation Construction and Explanation

In this section, a SISO single-mode system is generated via the MATLAB SIMULINK in order to validate SA approach. The model of this control system is as same as the model which is used in the last chapter with an aim to compare the optimization performance between GA and SA approaches. The SA optimization operation is performed and timed via the MATLAB. The MATLAB script can refer to Appendix A. After optimizing the gain and generating the optimized the controller, the compare between the uncompensated and compensated by the optimized compensator system responses is obtained.

The subsystem of the controller is shown in the Figure 6.3.1.

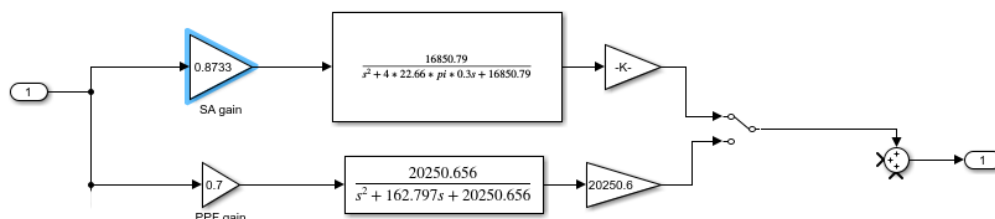


Figure 6.3.1 Subsystem of the controller

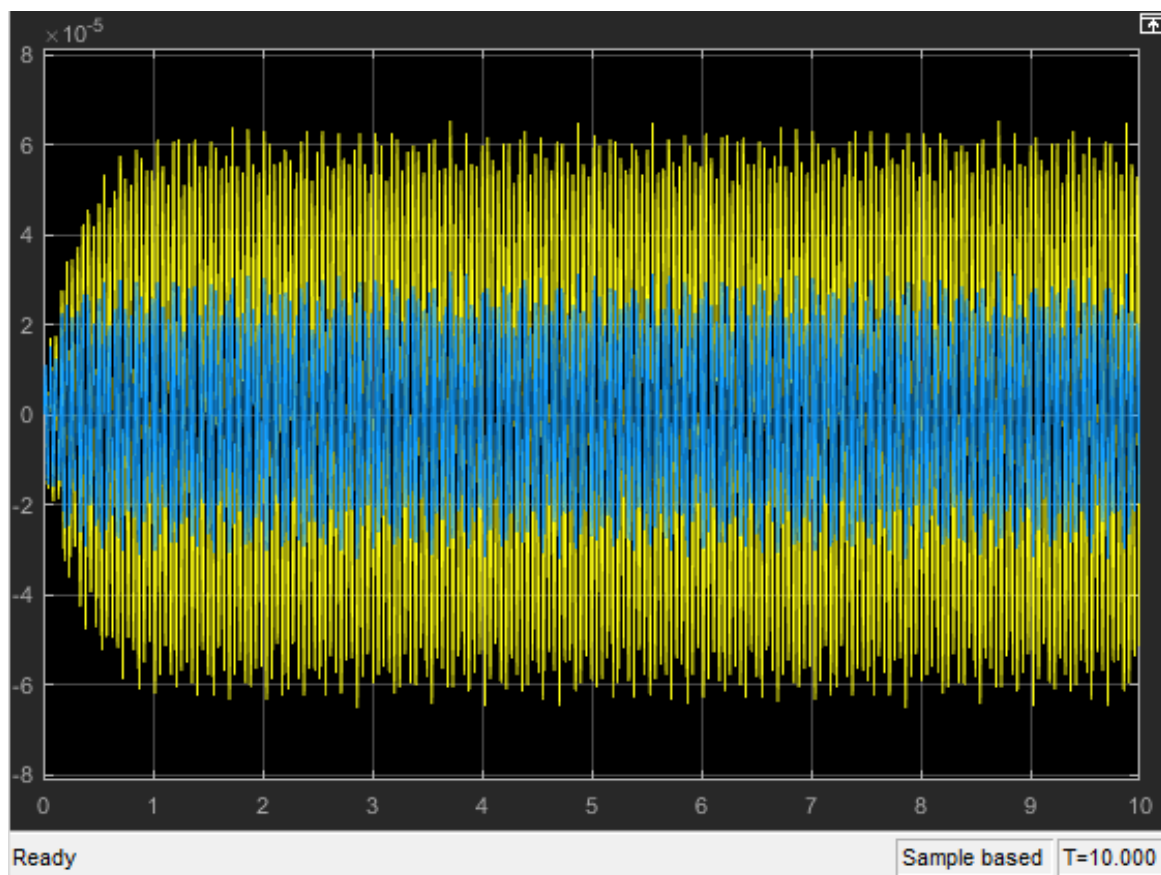
By using the MATLAB software, the gain of the new controller is optimized, the time of the computation is show in the Figure 6.3.2.

Function Name	Calls	Total Time	Self Time*	Total Time Plot (dark band = self time)
ssfsa	1	11.966 s	0.006 s	
normssf	16	11.960 s	0.110 s	

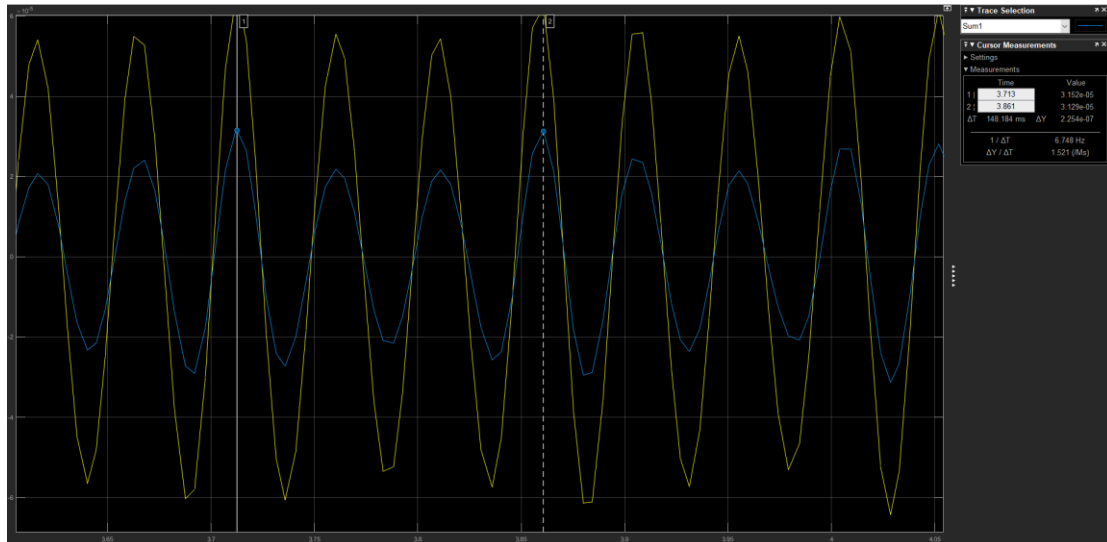
Figure 6.3.2 Computation time of the GA optimization operation

Since the SA optimization operation and GA optimization operation is performed via different computer, the computation time of running ‘normssf’ MATLAB script is various due to the different computer performance. If SA optimization operation is performed via the same computer, which means the computation time of the subfunction of ‘normssf’ is the same, the computation time should around 0.349 seconds.

After optimizing the gain of the corresponding controller, the new optimized controller is switched on to replace the pre-designed controller. The compare between the uncompensated and compensated by the new optimized controller systems is shown in the Figure 6.3.3.



(a)



(b)

Figure 6.3.3 Responses of the original and optimized controller-controlled system

In the Figure 6.3.3 (a), the plot refers to the responses of original system and compensated system. And the Figure 6.3.3 (b) is the zoomed out and scaled version. According to the Figures 5.3.3 and 6.3.3, the control performances of pre-designed controller and optimized adaptive controller is summarized in the Table 6.1.

Table 6.1 Control performance SISO single-mode control system optimized via SA

Controller	Attenuation
Pre-designed controller	4.37 dB
Optimized adaptive controller	6.42dB

According to the Table 6.1, a further 2.04 dB attenuation can be achieved by using the SA optimized adaptive controller.

In conclusion, in terms of the computation time, GA is obviously required more times of the fitness evaluation operations; hence, online optimization via GA method is performed slower than via SA method. However, the advantage of GA is its higher ability on the global solution searching, which above GA can provide more effective optimized parameters of the compensators.

Chapter 7 : Conceptual Optimization Validation

Sometimes, equipment or instruments are impacted by a single and monotonous disturbance from the working environment, such as the influence caused by a fixed frequency electronic motor. However, in most of situations, the number of the disturbance is greater than one; therefore, there would be several disturbances whose frequencies are as same as natural frequencies corresponding to different modes. Hence, single-mode and multi-mode configurations are necessary. Based on the adaptive control system design aim and the requirements of the online optimization operations, an adaptive control system via Genetic algorithm(GA) and Simulated Annealing(SA) online optimization approaches is designed and tested in the Matlab Simulink. In this chapter, two configurations (namely, single-mode configuration - controlling the first mode only, multi-mode configuration - controlling the first three modes of the real system, respectively) are constructed for validation.

According to the GA and SA optimization theory, the closed-loop transfer function of the adaptive control system is required; hence, the estimation operation of the current structure is carried out firstly. Secondly, a pre-designed controller is selected. Then, some of parameters of the controller are modified directly based on the estimated structure, and others are optimized online via GA and SA approaches. Finally, the pre-designed controller is replaced by the new controller when the new controller is finalized designed and optimized. Based on the online optimization strategy developed in the chapter 4, the procedures of online optimization of the adaptive control system are shown in the Figure 7.1.

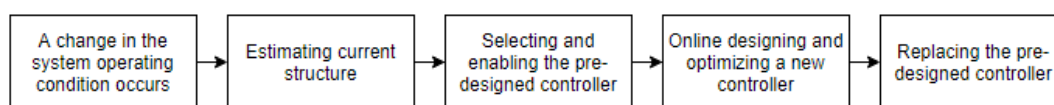


Figure 7.1 The block diagram of the adaptive control system with online optimization operation

7.1 Online optimization of the adaptive control system via single-mode configuration

In this section, the adaptive control system is designed and optimized for the first mode of the plate only. The control system is performed as three inputs three outputs system. But the plate is considered with its first mode in the resonate response. Hence, the compensator parameter

that needs to be optimized is the first gain only. The SIMULINK model of this single-mode configuration is shown as follows. Figure 7.1.1 shows whole the adaptive optimization control system. Figure 7.1.2 shows the subsystem of the system estimation. Figure 7.1.3 shows the subsystem of the online calculation. Figure 7.1.4 shows the subsystem of the controller.

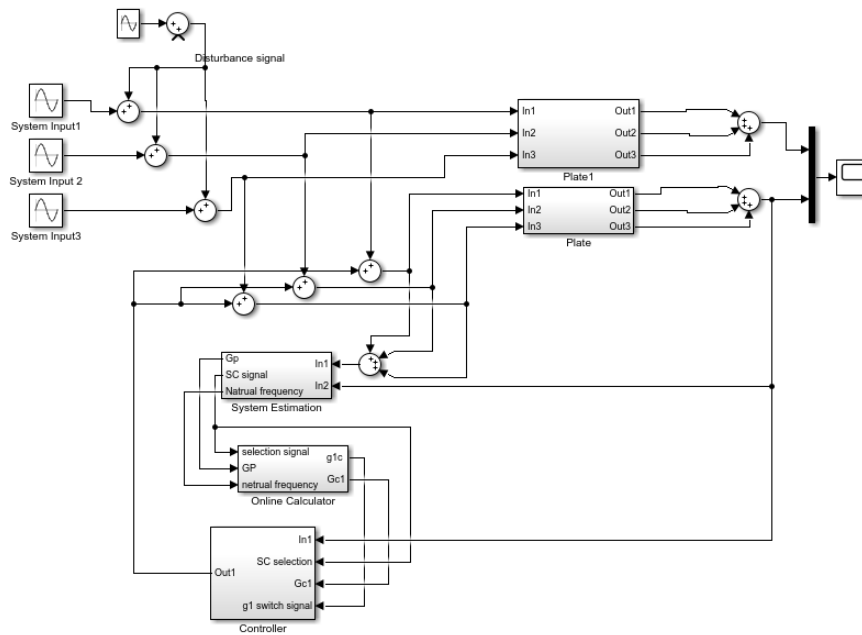


Figure 7.1.1 The adaptive optimization control system for single-mode configuration

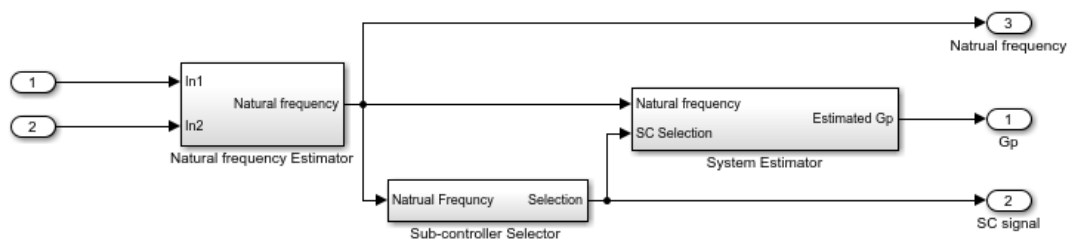


Figure 7.1.2 The subsystem of the system estimation

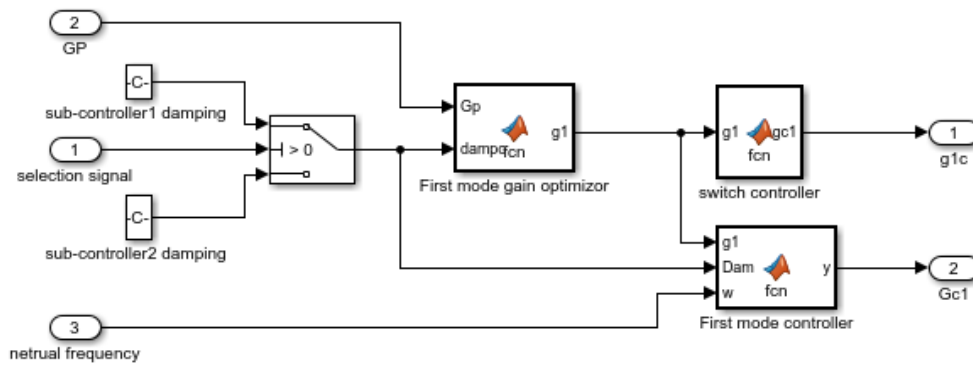


Figure 7.1.3 The subsystem of the online calculation

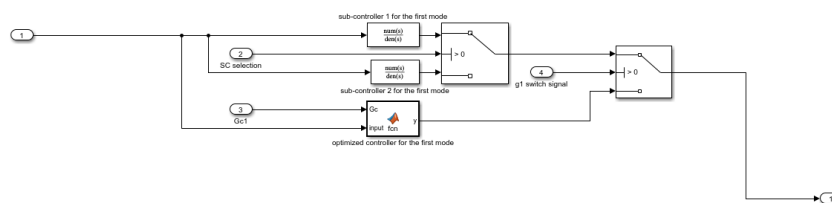
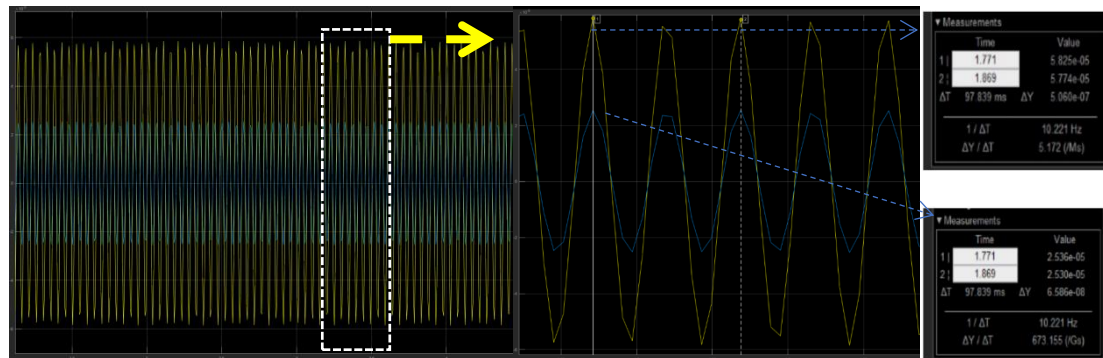


Figure 7.1.4 The subsystem of the controller

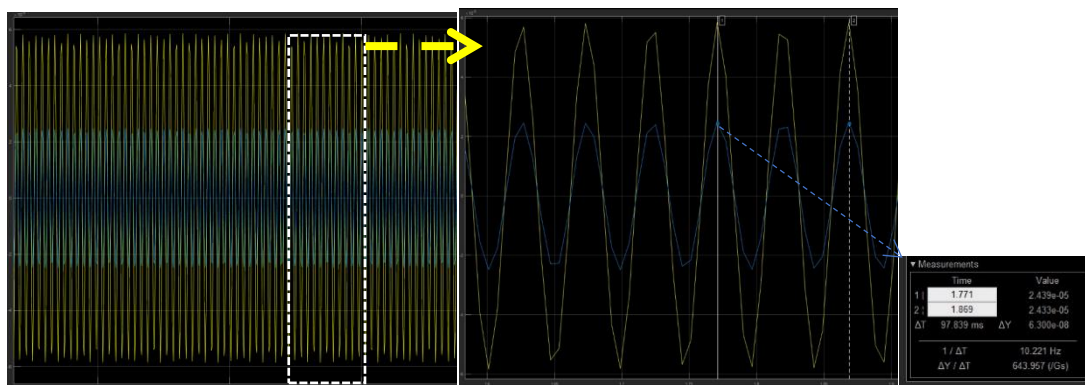
In the adaptive optimization control system (Figure 7.1.1), the inputs from 1 to 3 are zero as the initial condition of the plate. The input 4 is set as the disturbance and connected with both original plate and compensated plate. The outputs signal of these two plates are compared in the scope. In the subsystem of the system estimation (Figure 7.1.2), by using the inputs signals and out puts signals, the natural frequency is firstly estimated, and then, based on the estimated result, the pre-designed controller is selected followed by the structure estimation. The selection as one output signal is sent to the online calculator block and the controller block with the aim of providing a pre-designed controller of the compensated system. And the estimated structure as the other output is sent to the online calculator. In the online calculation subsystem (Figure7.1.3), with inputs, pre-designed controller selection signal and estimated structure information, the gain of the controller is optimized via GA and SA approaches, subsequently, as one of outputs, the switch signal is enabled till the optimized controller (the other output) is generated and send to the controller block. In the controller subsystem (Figure 7.1.4), two pre-designed controllers are stored. As soon as the selection signal is received, one of these two controllers is selected and performed until a new optimized controller is generated. The

MATLAB script of the pre-designed controller selection, the estimation of the structure, the optimization of gain and the generation of the optimized controller can refer to Appendix A.

After running the simulation, the outputs of these two plates are compared in the scope which is shown in the Figure 7.1.5.



(a)



(b)

Figure 7.1.5 Simulation result of single-mode adaptive control optimization system

According to the Figure 7.1.5(a), compared with uncompensated system, the compensated system with optimized controller via SA approach can achieve 7.217dB attenuation.

According to the Figure 7.1.5(b), compared with uncompensated system, the compensated system with optimized controller via GA approach can achieve 7.54dB attenuation.

7.2 Online optimization of the adaptive control system via multi-mode configuration

In this section, the adaptive optimization control system is simulated with aim of controlling the first three modes of the vibration. Compared with the single-mode configuration, number of the controllers increases to three, and the gain of each controller is required to optimized in this configuration. To take into account the possible spill-over effect that high frequencies may introduce to low frequencies, the controller gain for the highest mode of concern is optimized first, followed by the gains of the subsequent lower modes of concern.

In order to obtain the computation time of each approach, a non-automatic online optimization simulation is built. The structure of this system is shown in the Figure 7.2.1.

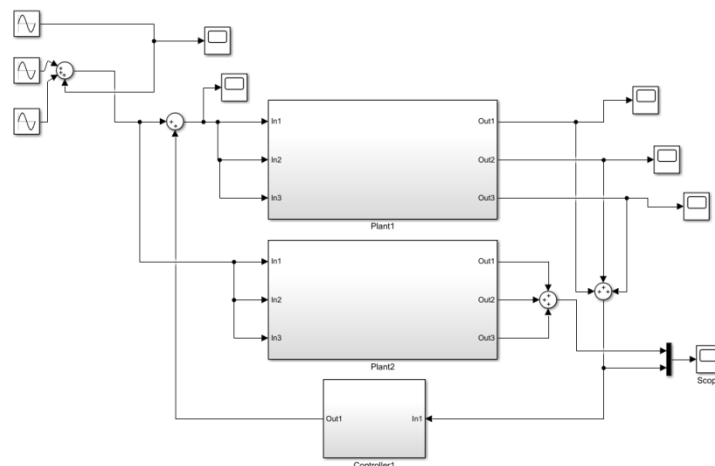


Figure 7.2.1 Block diagram of the control system in the MIMO configuration

In this configuration, plate is already estimated. According to the estimated information, the designed and optimized controller in unloaded working condition is selected as the sub-controller. In order to evaluating the fitness of GA approach and the objective value of SA approach, H^∞ computation function is generated and stored in the MATLAB script. According to the online optimization strategy which is developed in the chapter 4, the gains are optimized one by one; therefore, MATLAB scripts of the GA and SA are not modified.

The subsystem of the controller is shown in the Figure 7.2.2.

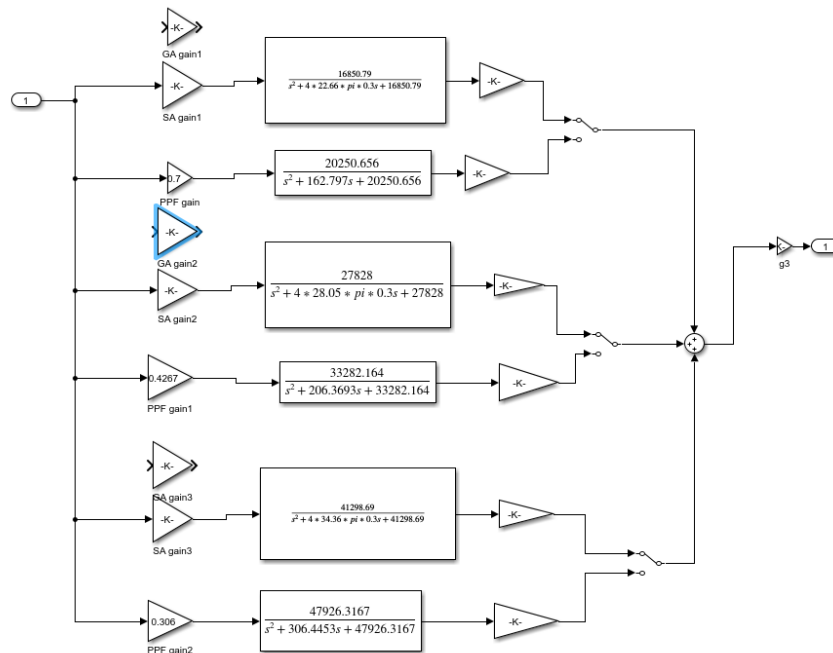


Figure 7.2.2 Block diagram of the controller subsystem

The response of the system compensated by pre-designed controllers is shown in the Figure7.2.3.

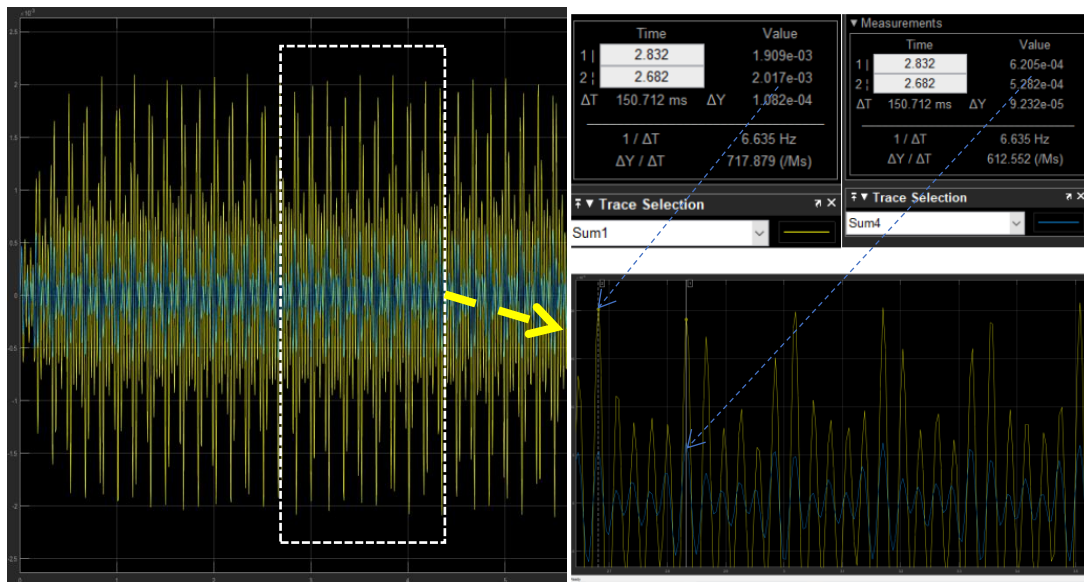


Figure 7.2.3 Response of the non-optimized control system

Then, the optimization operations are performed. The order of the optimization of gains is from gain3 to gain1. After the gain3 is optimized via GA and SA approaches, the corresponding controller is switched on to replace the pre-designed controller. The computation time via GA and SA approaches is shown in the Figure 7.2.4. The response plot is shown in the Figure 7.2.5.

Chapter 7: Conceptual Optimization Validation

Function Name	Calls	Total Time	Self Time*	Total Time Plot (dark band = self time)
GA	1	144.733 s	1.090 s	
normh	200	143.642 s	1.247 s	

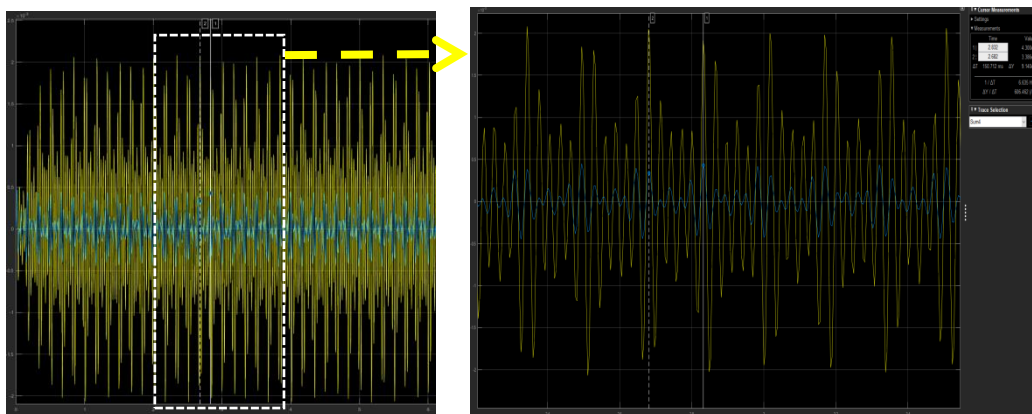
(a)

Function Name	Calls	Total Time	Self Time*	Total Time Plot (dark band = self time)
allprops	23932	6.897 s	6.897 s	
normh	31	6.407 s	0.205 s	

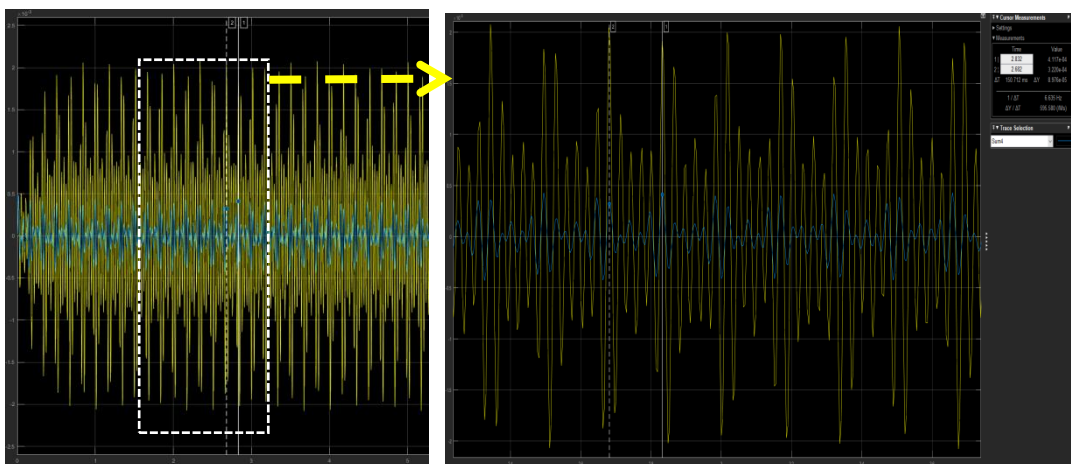
(b)

Figure 7.2.4 Computation time of gain3 optimization

The Figure 7.2.4(a) shows the computation time of the optimization operation via GA approach. The Figure 7.2.4(b) represents the computation time of the gain3 optimization operation via SA approach.



(a)



(b)

Figure 7.2.5 Responses of the control system with optimized third mode controller via GA and SA optimization approaches.

The Figure 7.2.5 (a) and (b) represents the response of the closed-loop compensated system. The controllers are consisted by two pre-designed controllers of the first two modes and one optimized adaptive controller of the third mode by using GA and SA optimization methods, respectively.

Based on the above control system, the optimization operation for the second mode controller is processed. The computation time of GA and SA optimization operations are shown in the Figure 7.2.6.

Function Name	Calls	Total Time	Self Time*	Total Time Plot (dark band = self time)
GA	1	141.203 s	1.145 s	
normh	200	140.058 s	1.198 s	

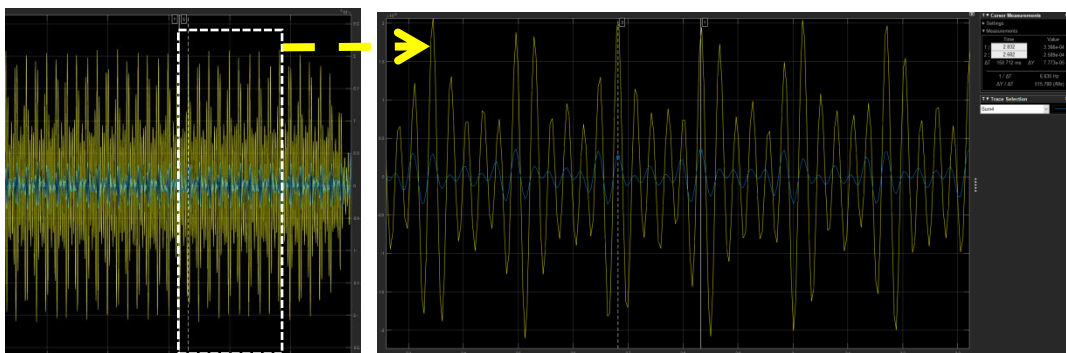
(a)

Function Name	Calls	Total Time	Self Time*	Total Time Plot (dark band = self time)
allprops	17756	5.179 s	5.179 s	
normh	23	4.023 s	0.158 s	

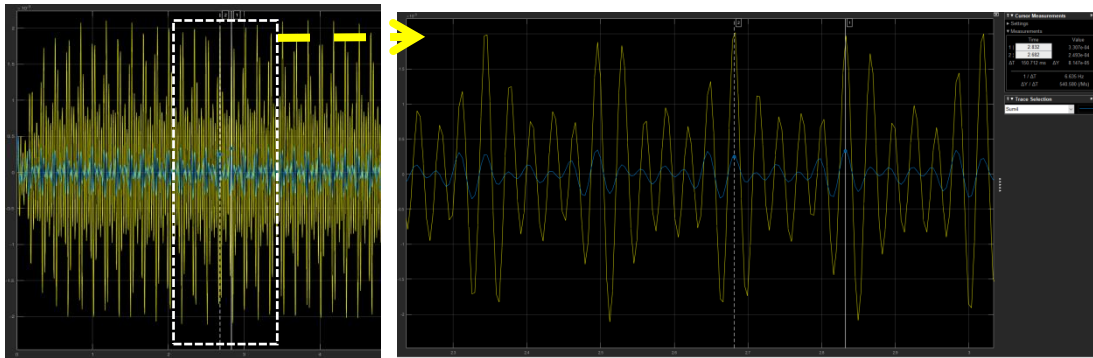
(b)

Figure 7.2.6 Computation time of gain2 optimization

The response of closed-loop compensated system is shown in the Figure 7.2.7.



(a)



(b)

Figure 7.2.7 Responses of the control system with optimized second and third modes controllers via GA and SA optimization approaches.

The Figure 7.2.7 (a) and (b) represents the response of the closed-loop compensated system. The controllers are consisted by one pre-designed controllers of the first mode and two optimized adaptive controllers of the second and third modes by using GA and SA optimization methods, respectively.

Finally, the first mode controller is optimized via GA and SA approaches. The computation time of these two optimization methods is shown in the Figure 7.2.8.

Function Name	Calls	Total Time	Self Time*	Total Time Plot (dark band = self time)
GA	1	142.536 s	1.123 s	
normh	200	141.412 s	1.193 s	

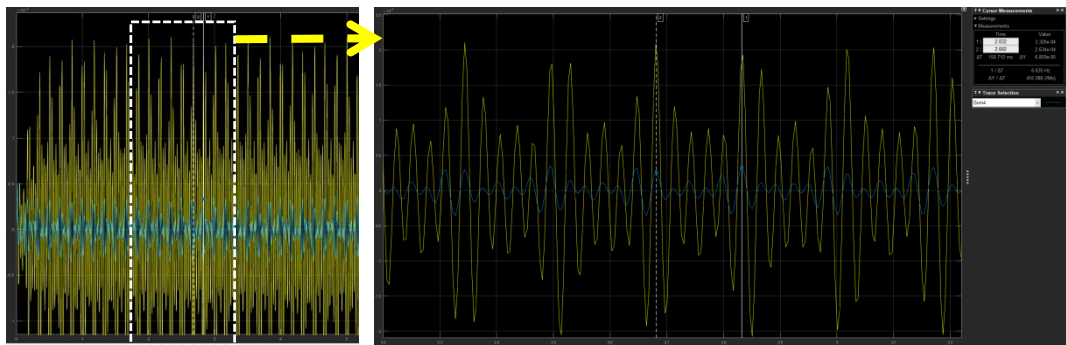
(a)

Function Name	Calls	Total Time	Self Time*	Total Time Plot (dark band = self time)
allprops	56356	16.082 s	16.082 s	
InputOutputModel.subsref	61612	6.775 s	4.925 s	
normh	73	4.798 s	0.451 s	

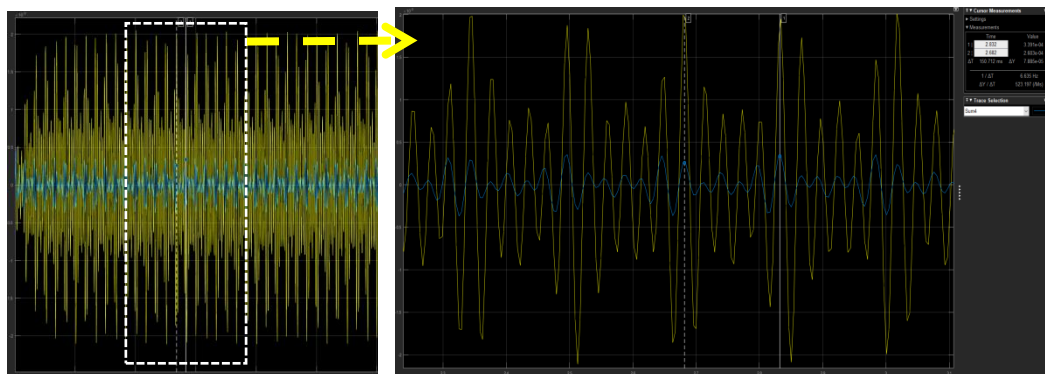
(b)

Figure 7.2.8 Computation time of gain1 optimization

The response of closed-loop compensated system is shown in the Figure 7.2.9.



(a)



(b)

Figure 7.2.9 Responses of the control system with optimized first three modes controllers via GA and SA optimization approaches.

So far, all of first three modes adaptive controllers are optimized and all of the pre-designed controllers are replaced. According to the Figures from 7.2.3 to 7.3.9., the computation time and control performance of optimized control system via GA and SA methods are summarized in the Table 7.1 and Table 7.2, respectively.

Table 7.1 The optimization performance of GA approach

		Amplitude (10^{-4})	Magnitude (dB)	Time cost of optimization for correspond- ing gain (second)	Attenuation (dB)
System	None controller	20.17	-53.91	-	-

Pre-designed controllers only	6.205	-64.14	-	10.23
optimized last two modes controller	4.117	-67.71	144.733	13.80
optimized last two modes controllers	3.366	-69.45	141.203	15.54
optimized first three modes controllers	3.320	-69.57	142.536	15.66

Table 7.2 The optimization performance of SA approach

		Amplitude (10 ⁻⁴)	Magnitude (dB)	Time cost of optimization for corresponding gain (second)	Attenuation (dB)
System controllers' configuration	None controller	20.17	-53.91	-	-
	Pre-designed controllers only	6.205	-64.14	-	10.23
	optimized the first	4.300	-67.33	6.897	13.42

Chapter 7: Conceptual Optimization Validation

mode controller					
optimized last two modes controllers	3.391	-69.393	5.179	15.48	
optimized first three modes controllers	3.370	-69.44	16.082	15.53	

According to the Tables 7.1 and 7.2, a further 5.20 dB attenuation can be achieved by using the SA optimization method in 28.158 seconds. Although a further 5.43 dB attenuation is achievable by using the GA optimization method, the total computation time is 428.472 seconds.

Due to the fact that SA requires much less number of iterations, the computation time can be effectively saved. However, as a kind of greedy algorithms, SA is hard to provide solution as good as what GA generates.

Chapter 8 : Conclusion

In most control systems, the target object is a dynamic structure; therefore, an adaptive control system always plays a very important role. Being different from non-adaptive control system, adaptive control system has to face with an unknown structure and needs to have a fast response ability.

In this project, a multi-input multi-output (MIMO) vibration cancellation control system is developed to remove and multiple resonant modes of the vibration which is caused by unwanted disturbances. This adaptive MIMO control system is constituted by an effective parameter estimator, an online calculator and an adaptive controller. Based on the estimation results, the adaptive controller which receives appropriate parameters calculated by the online calculator will be able to control the system successfully. The Positive Position Feedback controller is chosen as an adaptive vibration controller for the system because it has quick roll-off property at high frequencies, stability of the corresponding closed-loop system and high robustness.

Before developing the control system, the system identification is required because the mathematical model established of the target structure has a widespread application through whole course of the system development. Since first three modes mainly dominate the effect from the resonant, the PPF controller is designed to focus on the first three modes vibration cancellation, and only first three modes are covered in system identification. A laboratory structure is constituted by three sensors and actuators pairs, two plates, a base plate and a flexible plate as a top plate and one disturbance transducer. Based on the modal analysis theory and utilizing physical experiment, the frequency response function matrix of the plant can be obtained. As a result, there are twenty-seven frequency response transfer functions and each function are differently labeled by the number of input, output and the order of the mode. These functions which share same output and order of the mode are combined.

A widely recognized defect of the control optimization, calculating the most suitable parameters of the controller, is that it spends amounts of time which is not acceptable for online control system. The switching-sub-model method, as a sub-optimization stage, can be used to provide time for succedent online calculation. In this stage, these optimized parameters of the

controller have been stored in the controller subsystem in order to be employed as emergency control parameters.

To further optimize the PPF controller, it is required to search for better parameters of PPF controller. Firstly, the estimation of the structure is processed because of vary loading conditions based on the relationship between dynamic natural frequency and shaking model shape. After estimating the mathematical model of the current structure, according to the characteristics of the PPF controller, the controller frequency and value of damping ratio are chosen, and PPF controller transfer function matrix will be set with variable controller gain set. With estimated target object model and controller, H_{∞} norm is able to be built as a trial function to measure control result caused by PPF controller constituted by different control gain sets. Because our control system is built to control first three modes, and PPF controller is able to be optimized one by one. Due to PPF controller which is a low-pass filter, the optimization is processed from the third mode to the first mode, Genetic Algorithm(GA) method can search optimized gain values, but the cost of calculating time cannot be ignored because H_{∞} norm is required to be calculated N times (N is the size of population set in GA) in one generation. This step is repeated until finish all generations. For the sake of calculation in an acceptable period of time, N , G (the number of generation), and aberration rate are set as small as possible, and also keep the ability to find an effect gain set of the controller. The other method, Simulated Annealing (SA) is also used to search the controller gain set. SA method can provide the gain value which results in lowest H_{∞} norm in the range of controller gain with less number of calculation steps.

The simulation is built with 4 main parts: target structure, online estimator, online calculator and PPF controller. The plate is simulated based on the mathematical model with three inputs and three outputs as well as a disturbance provider which is added as an energy source. The online estimator is designed to estimate the nature frequency of the plate when it changed due to the vary loading condition. The online calculator uses the result from estimator and calculate the most effect gains and then sent them to the controller. PPF controller part has three inputs from the plate and provide corresponding damping ratio for each mode. By running the simulation and observing the result, the speed of the calculation is acceptable, and in the most of time, this adaptive control system can control the dynamic plate with acceptable responds. There also exists possibility of only use the sub-optimization result because the best solution of controller gains exists in the first part of range which is missed by SA optimizer and provide

less effect gain values than what sub-optimization part provides; moreover, the researching result of GA optimizer is also worse than SA optimizer.

Through the PPF controller offline optimization algorithm, the simulation of the control systems which includes optimized offline under two conditions are designed firstly. Next, the simulation of target structure is modified due to different loading conditions. PPF controller is designed with one of the previous parameter sets, with an aim to validate the control effect with sub-optimized controller. Then, the simulations of GA and SA optimizer are designed respectively. In order to observe the optimization effect through sub-optimized, GA and SA optimizer, the mathematical model under half loaded condition is estimated. In this condition, compared with the open-loop, the response magnitude can be reduced by sub-optimized control system by 10.23dB. Subsequently, the control system optimized by GA and SA optimizer is designed and observed. From the result, a further 5.20 dB attenuation can be achieved by using the SA optimization method in 28.158 seconds. Although a further 5.43 dB attenuation is achievable by using the GA optimization method, the total computation time is 428.472 seconds. In terms of the computation time, GA is obviously required more times of the fitness evaluation operations; hence, online optimization via GA method is performed slower than via SA method. However, the advantage of GA is its higher ability on the global solution searching, which above GA can provide more effective optimized parameters of the compensators.

Chapter 9 : Future Work

In this chapter, the two-possible developed online optimization strategies, directly observing evaluation approach and optimization approach via Quadratic optimal control theory, are discussed. Since the current computation time is still too much to effectively optimized a time-varying system.

9.1 Directly observing evaluation approach

According to the figures related to the computation time, the evaluation operations spend most computation time during online optimization. Hence, a developed evaluation approach of the gain in each iteration can improve the online optimization speed. In the section, a possible developed online optimization strategy is discussed. In this strategy, the gain is evaluated based on the closed-loop response which can be directly obtained from the experimental equipment. In this project, the gain is evaluated by computing the value of H^∞ of the closed-loop transfer function matrix to evaluate each gain during the optimization operation. Evaluating of gain via observation has almost none computation. The core concept of this evaluation approach is that a higher maximal amplitude leads to a lower performance of the control system with current gain. The challenge of this evaluation approach is sampling period design. To correctly evaluate the parameters of the controller, the maximal amplitude of the response should be related to the current control system only. Therefore, the sampling frequency should be set as a fraction of the greatest common divisor of all estimated natural frequencies or smallest natural frequency. Considering the effects of last control system and inertia, the valid demarcation line in each sampling period cycle is required to be design as well. With a designed valid demarcation line and sampling period, the maximal amplitude can be used to evaluate the performance of the control system constituted by current parameters in a time period that is from valid demarcation line to the end of sampling cycle.

9.2 Online optimization via Quadratic optimal control theory

In this section, a developed online optimization strategy is presented. The controller gains can be optimized directly by applying the Quadratic optimal control theory rather than by globally searching the best solution in each parameters' ranges [13]. According to the Quadratic optimal control theory, a state-space representation of the closed-loop system is required to be

developed firstly. Based on the equations (4.2.4) and (4.2.5), the state of the closed-loop system is defined as:

$$V(t) = \begin{bmatrix} X(t) \\ \dot{X}(t) \\ Z(t) \\ \dot{Z}(t) \end{bmatrix} \quad (9.2.1)$$

The state-space representation is:

$$\dot{V}(t) = \tilde{A}V(t) + \tilde{B}U(t) \quad (9.2.2)$$

$$Y(t) = \tilde{C}V(t) \quad (9.2.3)$$

, where

$$\tilde{A} = \begin{bmatrix} 0 & I & 0 & 0 \\ -W^2 & \psi & 0 & 0 \\ 0 & 0 & 0 & I \\ W_c^2 C_i & 0 & -W_c^2 & \psi_c \end{bmatrix} \quad \tilde{B} = \begin{bmatrix} 0 \\ C_i \\ 0 \\ 0 \end{bmatrix} \quad \tilde{C} = [0 \quad C_o \quad 0 \quad 0]$$

Hence, the Quadratic Performance Index of this system can be represented as:

$$J = \int_0^{\infty} [V(t)^T QV(t) + U(t)^T RU(t)] dt \quad (9.2.4)$$

, where Q and R are state weighting matrix and input weighting matrix, respectively.

The linear quadratic control can be described by:

$$U(t) = KV(t) \quad (9.2.5)$$

, where K is the quadratic optimal state-feedback gain matrix.

With the optimal control goal, K is figured out such that J is minimal. K can be calculated by equation (9.2.6) [1].

$$K = R^{-1} \tilde{B}^T P \quad (9.2.6)$$

, where P is the solution of the Riccati equation (9.2.7)

$$\tilde{A}^T P + P \tilde{A} - P \tilde{B} R^{-1} \tilde{B}^T P + Q \quad (9.2.7)$$

According to the structure of the PPF controller, the output signal matrix can be represented as:

$$U(t) = \tilde{K} Z \quad (9.2.8)$$

, where $\tilde{K} = G W_c^2$

If there exists a transfer matrix T that ensures equation (9.2.9) hold, combining the equations (9.2.5) and (9.2.8), the equation (9.2.10) is able to calculate each gain of the gain matrix.

$$TZ = V \quad (9.2.9)$$

$$KT = G W_c^2 \quad (9.2.10)$$

Moreover, the control system can be optimized to be much faster because the parameters are generated by the several calculation operations rather than multiple iterations searching and selecting operations

Due to time constraints, the transfer matrix T is not figured out currently. As a future work, calculation of the matrix T is the main point.

Appendix A: MATLAB Code

The MATLAB codes for each section are kept within the Advanced Control Research Group, Flinders University. The MATLAB codes can be provided upon request.

Bibliography

- [1] Sun, L., Wu, G. (2010). Application and Optimize Design of Active Disturbance Rejection Controller. EMCA.
- [2] Yang, W. and Boyd, S. (2010). Fast model predictive control using online optimization[J]. IEEE Transactions on control systems technology,18(2), pp. 267-278.
- [3] Wills, D. and Fleming, A. (2008). Model predictive control applied to constraint handling in active noise and vibration control. IEEE Transactions on Control Systems Technology,16(1), pp. 3-12.
- [4] Goldfarb, D. and Idnani, A. (1983), A numerically stable dual method for solving strictly convex quadratic programs, Math. Program, 27(1), pp. 1–33, 1983.
- [5] M. J. D. Powell, (1985), On the quadratic programming Algorithm of Goldfarb and Idnani, Math. Program. Study, vol. 25, pp. 46–61.
- [6] Schittkowski, K. , QL: A fortran code for convex quadratic programming—Users's guide, Dept. Math., Univ. Bayreuth, Bayreuth, Germany,2003.
- [7] Tanguy, Morvan R and Vilbé P. Online optimization of the time scale in adaptive Laguerre-based filters[J]. IEEE Transactions on Signal Processing, 48(4): 1184-1187,2000
- [8] G. Katta Linear complementarity, linear and nonlinear programming. Sigma Series in Applied Mathematics,Heldermann Verlag. 1988, pp. xlviii+629 pp. ISBN 3-88538-403-5.
- [9] J. Delbos and J. Gilbert Global linear convergence of an augmented Lagrangian algorithm for solving convex quadratic optimization problems. Journal of Convex Analysis, 2005, pp. 45–69.
- [10] A. Forsgren, E. Gill and E. Wong Active-set methods for convex quadratic programming[J], 2015, pp.1-3.
- [11] C. Gionata, and A. Bemporad. Exact complexity certification of active-set methods for quadratic programming. IEEE Transactions on Automatic Control 62.12 ,2017, pp. 6094-6109.
- [12] M. Cannon, B. Kouvaritakis and J. Rossiter, Efficient active set optimization in triple mode MPC[J]. IEEE Transactions on Automatic Control, 2001, pp. 1307-1312.

Bibliography

- [13] Michael, A. and Peter, L. (1990), *Optimal control: an instruction to the theory and its application*, McGowan-Hill.
- [14] Sun Y. and Wang Z., *The Application of Genetic Algorithm in Optimization*, *Control and Decision*, vol. 11, no. 4, July 1996.
- [15] Li J., Liu H., Zhang L., *Optimal Placement of Active Members in Active Vibration Control of Adaptive TR USS Structure*, *Acta Aeronautical et Astronautical Sinica*, vol. 17, no.6, Nov. 1996.
- [16] Ji G., *Survey On Genetic Algorithm*, *Computer Applications and Software*, vol. 21, no. 2, Feb. 2004.
- [17] Chen, W., Chu, F. and Shao, Z. (2010), *Stepwise Optimal Design of Active Disturbances Rejection Vibration Controller for Intelligent Truss Structure Based on Adaptive Genetic Algorithm*, *Journal of Mechanical Engineering*, 46(7).
- [18] Li, J., Wei, F. and Liu, W. (2009), *Seismic reliability optimization of water distribution networks with simulated annealing algorithms*, *Journal of Earthquake Engineering and Engineering Vibration*, 29(3).
- [19] Vanlanduit, P., Verboven, P. and Guillaume, J. (2003), *An automatic frequency domain modal parameter estimation algorithm*, *Journal of Sound and Vibration*, pp. 647–661.
- [20] Avitabile, P. (2001), *Experimental modal analysis*, *Sound and vibration*, 35(1), pp.20-31.
- [21] Lim, T., Bosse, A. and Shalom, F., (1996), *Structural damage detection using real-time modal parameter identification algorithm*, *AIAA Journal*.
- [22] Bosse, A., Lim, T. and Stuart, S., (2000), *Modal filters and neural networks for adaptive vibration control*, *Journal of Vibration and Control*, pp.631-648.
- [23] Rew, K., J. Han, and Lee, I., (2000), *Adaptive multi-modal vibration control of wing-like composite structure using adaptive positive position feedback*, *AIAA Journal*, pp.664–673.
- [24] Du L., Yan Y., Wang D., *Optimal Disposition of Actuator in Active Vibration Control of Intelligent Structures Based on Genetic Algorithms*, *Journal of Northeastern University (Natural Science)*, vol. 20, no. 2, Apr. 1999.
- [25] Yuan Q., Huo, M., Qi N., Cao S. and Xiao Y., *Vibration control for large flexible maneuvering spacecraft using modified positive position feedback*, *Journal of Beijing University of Aeronautics and Astronautics*, vol. 44, no. 2, Feb. 2018.

Bibliography

- [26] Lou J., Wei Y., Yang Y., Xie F. and Zhao X., Modified Multi-mode positive position feedback controller for active vibration control of a smart flexible structure, *Journal of Vibration and Shock*, vol. 34, no. 10, 2015.
- [27] Hu J. and Zhang X., "Active Vibration Control and Its Simulation of a Novel 2-DoF Flexible Parallel Manipulator," *China Mechanical Engineering*, vol. 21, no. 17, Sep. 2010
- [28] Chen W., Chu F. and Yan S., "Stepwise Optimal Design of Active Disturbances Rejection Vibration Controller for Intelligent Truss Structure Based on Adaptive Genetic Algorithm," *Journal of Mechanical Engineering*, vol.46, no.7, Apr. 2010.
- [29] Lu, L. and Yao, B., (2014), Online constrained optimization based adaptive robust control of a class of MIMO nonlinear systems with matched uncertainties and input/state constraints, *Automatica*, 50(3), pp.864-873.
- [30] Lu, L. and Yao, B., (2011), Globally stable fast-tracking control of a chain of integrators with input saturation and disturbances: a holistic approach, In *Proceedings of American control conference*, pp. 4434–4439.
- [31] Pratama, G., (2010), Characterization of vibration of two-dimensional rectangular plate (honours thesis, Flinders University-Adelaide Australia).
- [32] Chen, Q., (2016), Vibration Cancellation in Plate Structures. (honours thesis, Flinders University-Adelaide Australia).
- [33] Yu, S., 2012. Mechanical Structure Modelling and Vibration Control (bachelor thesis, Flinders University-Adelaide Australia).
- [34] Liu L., Lu W. and Mou S., "Switching Multiple Model adaptive control based on online optimization," *Control and Design*, vol. 17, no.4, July 2002.
- [35] Zhang, P. and He, F. (2017). MIMO PPF Active Vibration Control of Asymmetrical Plate Structures. In: *The 13th IEEE Conference on Industrial Electronics and Applications*. Wuhan.
- [36] Ewins, D.J., (1984). *Modal testing: theory and practice* (Vol. 15). Letchworth: Research studies press.
- [37] Wang X., "Calculation of the Eigen-Frequencies and Designing of the Absorbers of a Flexible Beam with Tip Mass," *Journal of Southeast University*, vol. 27, no. 5, Sept. 1997.